Compositional Structures in Two Batholiths of Circumpacific North America

GEOLOGICAL SURVEY PROFESSIONAL PAPER 574-H

Compositional Structures in Two Batholiths of Circumpacific North America

By A. T. MIESCH *and* BRUCE L. REED

STATISTICAL STUDIES IN FIELD GEOCHEMISTRY

GEOLOGICAL SURVEY PROFESSIONAL PAPER 574-H

A mathematical analysis of chemical data on 386 samples of granitic rocks from the Sierra Nevada and Alaska-Aleutian Range batholiths, and discussion of the petrogenetic implications of the results

UNITED STATES GOVERNMENT PRINTING OFFICE, WASHINGTON: 1979

UNITED STATES DEPARTMENT OF THE INTERIOR

CECIL D. ANDRUS, *Secretary*

GEOLOGICAL SURVEY

H. William Menard, *Director*

Library of Congress Cataloging in Publication Data
Miesch, Alfred T.
Compositional structures in two batholiths of circumpacific North America.
(Statistical studies in field geochemistry)
(Geological Survey Professional Paper 574-H)
Bibliography: p. 30
Supt. of Docs. no.: I 19.16:574-H.
1. Batholiths—Sierra Nevada. Mountains. 2. Batholiths—Alaska—Aleutian Mountain Range.
3. Granite—Sierra Nevada Mountains. 4. Granite—Alaska—Aleutian Mountain Range. 5. Phase rule and equilibrium. 6. Multivariate analysis.
I. Reed, Bruce L., 1934- joint author. II. Title. III. Series. IV. Series: United States Geological Survey Professional Paper 574-H.
QE75.P9 no. 574-H [QE611.5.U6] [551.8'8] 557.3'08s 78-606014

For sale by the Superintendent of Documents, U.S. Government Printing Office
Washington, D.C. 20402
Stock Number 024-001-03184-1

CONTENTS

ILLUSTRATIONS

TABLES

COMPOSITIONAL STRUCTURES IN TWO BATHOLITHS OF CIRCUMPACIFIC NORTH AMERICA

By A. T. MIESCH and BRUCE L. REED

ABSTRACT

The compositional structure within an igneous body or cogenetic series depends on the number of end members that are required to account for a major part of its compositional variation. If a large part of the compositional variation can be accounted for by mixing of only a few materials (magmas or magmas and country rocks), the compositional structure is simple. Or, the compositional structure is simple if the variation can be explained by the separation of only a few mineral phases from a magma.

Factor-variance diagrams constructed from data on major oxide constituents in samples from the Sierra Nevada and Alaska-Aleutian Range batholiths show that these bodies have fairly simple compositional structures, and, therefore, probably resulted from a few processes that were dominant over others. There is no need to call on highly complex mechanisms of fractional crystallization, assimilation, or magma mixing to account for the oxide data. In fact, the relatively simple compositional structures of the batholiths make these processes seem unlikely.

Models containing three end members can account for most of the compositional variability in each batholith. One end member is a parent magma, or magma-source material, and the other two represent the extremes in a two-component range of mafic mineral assemblages that separated from the magma. The compositions of 228 samples from the Sierra Nevada batholith and of 158 samples from the Alaska-Aleutian Range batholith can be closely approximated as linear combinations of these end members. These approximations are somewhat improved for the Sierra Nevada if a fourth end member is used; the end member representing the magma, or magma-source material, is replaced by two end members that are apparently required to account for variation in the composition of the magmas that formed across the present site of the batholith. The principal variation among these magmas is in K_2O content, which was slightly higher in magmas formed at a distance from the continental margin.

If it is assumed that the magmas were generated by partial melting of the crust or other material, the models may be used to estimate a range of compositions for the partial melts that formed each sample. The final composition of each sample was determined by the composition of this melt and by the composition of mafic mineral assemblages that were either retained in the melt after partial melting of the crust or precipitated from the melt during its ascension to the present site of each batholith. The melt compositions that are estimated on the assumption of minimum heat requirements correspond well with those that occur along cotectic lines on classical phase diagrams. Individual samples from the Alaska-Aleutian Range batholith required melting of 6 to 24 percent of the crust, with an average of about 9 percent melting. Most individual samples from the Sierra Nevada batholith require melting of 11 to 27 percent of the crust; the average degree of crustal melting required for individual groups of plutons (sequences) ranges from 17 to 21 percent.

Although the models developed for the two batholiths are not unique, they appear to be in accord with major geologic observations that bear on the batholiths' origins. Other models could be developed that would account equally well for the compositional variabilities; however, these other models would also have to account for the fairly simple compositional structures present in each of the batholiths.

INTRODUCTION

Almost all of the observed compositional variation in igneous rock bodies has resulted from processes of mixing or unmixing. Mixing occurs where country rock is incorporated into the magma or where two or more magmas or melts come into contact. Unmixing results from magmatic differentiation. Because nearly all of the variation results from mixing and unmixing, it is helpful to examine the variation by some kind of vector analysis. Vector systems constructed from chemical and mineralogical data on samples from an igneous body reflect the compositional structure of the body. The compositional structure depends on the kind of mixing and unmixing that occurred—that is, on the number of materials involved and the variations among the proportions added or separated.

The only mathematical difference between mixing and unmixing is in the signs of the mixing proportions. A rock may have formed by the mixing of, say, 0.6 parts of material x and 0.4 parts of material y. It may also have formed by the unmixing of 0.4 parts of material z from 1.4 parts of material x; that is, mixing of 1.4 parts material x and -0.4 parts material z. The only requirement is that the mixing proportions sum to unity. In the discussion to follow, the term mixing refers to either type of process, unless *mixing in positive proportions* or *unmixing* (separation) is specified.

The purpose of this report is to illustrate the concept of compositional structure, to discuss its bearing on in-

terpretation of the origin of igneous rocks, and to describe the compositional structures in major parts of the Sierra Nevada batholith of California and the Alaska-Aleutian Range batholith. The method of vector analysis employed is based on a form of *Q*-mode factor analysis originally described by Klovan and Imbrie (1971) and extended for use in geochemistry and petrology (Miesch, 1976a, 1976b). Computer programs for the extended *Q*-mode have been given by Klovan and Miesch (1976) and Miesch (1976c). An attempt will be made here to emplôy the methods and concepts of *Q*-mode analysis, and to describe the results in terms familiar to petrologists who have had little or no experience with factor analysis. Other readers may wish to consult the references cited and the appendix for additional details or mathematical clarification. Excellent introductions to the concepts and terminology of factor analysis methods in geology were given by Imbrie (1963) and Klovan (1975).

We are grateful to Paul C. Bateman for selecting the 228 analyses used in examination of the Sierra Nevada batholith and for helpful criticisms of early drafts of the manuscript. We also appreciate the helpful criticisms and suggestions provided by Z. E. Peterman, Priestley Toulmin 3d, and David R. Wones.

COMPOSITIONAL STRUCTURE

Multivariate statisticians commonly use the term *structure* in referring to the patterns of variation or order within a data matrix. If the variables represented in the matrix vary almost independently of one another, the matrix has little or no structure. If the variables are correlated at least some structure is present, and if the structure is pronounced it is possible that the information contained in the data matrix might be expressed approximately in a simpler matrix that could be more easily interpreted in terms of the subject matter problem. The oxide variables represented in petrologic data matrices always display some correlation with one another. Therefore, these variables can quite commonly be represented in alternative matrices with fewer columns, if the columns represent variables other than the original oxides, such as combinations of the oxides that may approximate or equal the compositions of rocks, magmas, and minerals. Thus, the term structure seems appropriate and useful for describing this property of petrologic data and the rock bodies that the data represent. Depending on the amounts of correlation present, the compositional structures may range from simple (pronounced) to complex (weak) and the structural complexity, in turn, determines the number of columns in the alternative data matrix. Of particular significance to the petrologist is the fact that this complexity determines the number of end members required to account for the compositional variation in the petrologic system.

In spite of the mathematical justification for use of the term *structure* in the connotation explained above, we recognize that the term may have misleading implications to geologists. The choice of terms may be poor for this reason, but no better term has come to mind.

Two hypothetical data matrices are given in tables 1 and 2. Corresponding constituent means and standard deviations are about the same from one matrix to the other. The main difference between the two is in the compositional structures they represent. The matrix in table 1 can be reproduced only by mixing seven end members; for example, by mixing the seven end-member compositions in table 3*A* in the proportions given in table 3*B*. In contrast, the data in table 2 may be reproduced exactly by mixing only three end members, such as those of table 4*A* in the proportions given in table 4*B*. The data in table 1, therefore, reflect a complex compositional structure, whereas the compositional structure represented by the data in table 2 is relatively simple. Complex compositional structures result from processes that have involved a large number of end members being mixed in variable proportions. Simple compositional structures result from mixing a relatively small number of end members, or conceivably, from mixing a larger number of end members in rather constant proportions. However, the latter process effectively reduces the number of end members; if two end members are always mixed in proportions of, say, 3 to 1, then the two end members are effectively only one.

TABLE 1.—*Hypothetical data reflecting a complex compositional structure*

Sample	Constituent (weight percent)						
	a	*b*	*c*	*d*	*e*	*f*	*g*
1	50.16	3.54	4.78	5.33	34.47	0.41	1.41
2	52.85	10.17	8.75	9.79	15.11	.75	2.58
3	16.53	9.40	4.31	5.34	61.70	1.14	1.58
4	30.45	15.61	.05	11.74	37.14	1.32	3.69
5	50.97	7.06	5.20	8.33	24.92	.56	2.96
6	63.25	10.84	3.32	10.05	9.58	.10	2.86
7	29.09	.25	4.17	6.53	57.09	.59	2.28
8	40.88	5.03	3.95	7.54	39.33	.73	2.54
9	44.22	14.85	8.77	9.54	17.44	1.68	3.50
10	32.55	14.90	7.40	11.59	29.57	0	4.00
Mean	41.1	9.2	5.1	8.6	32.6	.7	2.7
Standard deviation	13.2	4.9	2.5	2.2	16.3	.5	.8

TABLE 2.—*Hypothetical data reflecting a simple compositional structure*

Sample	Constituent (weight percent)						
	a	*b*	*c*	*d*	*e*	*f*	*g*
1	51.25	7.08	4.01	6.64	27.62	1.07	2.33
2	29.15	8.40	5.75	10.20	42.10	1.45	2.95
3	76.83	4.72	1.35	2.49	12.41	.46	1.74
4	53.08	14.46	9.68	6.61	12.47	2.57	1.13
5	49.60	15.50	10.60	7.20	13.20	2.80	1.10
6	31.41	2.44	1.05	9.63	51.47	.22	3.78
7	36.11	6.32	3.91	9.02	40.64	.99	3.01
8	47.77	8.12	4.93	7.23	28.35	1.30	2.30
9	54.73	6.04	3.09	6.05	26.89	.84	2.36
10	25.06	6.98	4.78	10.80	47.88	1.18	3.32
Mean	45.5	8.0	4.9	7.6	30.3	1.3	2.4
Standard deviation	14.7	3.9	3.0	2.3	14.0	.8	.8

TABLE 3.—*Some end-member compositions and mixing proportions for the data in table 1*

A. **End-member compositions (weight percent)**

End member	Constituent						
	a	*b*	*c*	*d*	*e*	*f*	*g*
A	68.1	4.8	4.3	8.9	10.8	0	3.1
B	28.0	.1	4.5	6.0	57.6	.8	3.0
C	29.0	12.3	1.2	13.1	36.2	1.6	6.6
D	38.0	1.6	1.4	9.1	44.7	.1	5.1
E	42.9	2.2	5.8	9.7	32.0	1.2	6.2
F	30.6	30.7	5.9	.6	29.4	.4	2.4
G	52.3	2.7	3.2	3.0	28.6	1.0	9.2

B. **Mixing proportions**

Sample	End member						
	A	*B*	*C*	*D*	*E*	*F*	*G*
1	0.8	1.0	0.1	-0.5	-0.5	0	0.1
2	.5	-.1	-.2	-.3	1.3	.3	-.5
3	0	1.3	.4	-.4	-.4	.2	-.1
4	.5	.6	1.3	-.4	-1.0	0	0
5	.6	.3	.1	-.2	.2	.1	-.1
6	1.0	-.1	.3	0	-.2	.1	-.1
7	.1	1.0	0	.1	-.1	0	-.1
8	.5	.8	.3	-.3	-.3	0	0
9	.4	.2	.3	-1.0	1.1	.3	-.3
10	-.5	-1.2	-.7	1.5	2.2	.7	-1.0

ROCK COMPOSITIONS REPRESENTED AS VECTORS

The method employed in *Q*-mode factor analysis for representing rock compositions as vectors can be illustrated best by considering a series of five entirely unrealistic rock samples composed of just SiO_2 and Al_2O_3. However, the hypothetical samples will be considered to have SiO_2 far in excess of Al_2O_3, as in common igneous rocks. The samples are represented as

TABLE 4.—*Some end-member compositions and mixing proportions for the data in table 2*

A. **End-member compositions (weight percent)**

End member	Constituent						
	a	*b*	*c*	*d*	*e*	*f*	*g*
A	49.6	15.5	10.6	7.2	13.2	2.8	1.1
B	84.4	5.1	1.4	1.3	5.9	.5	1.4
C	8.7	1.3	.9	13.2	71.0	.1	4.8

B. **Mixing proportions**

Sample	End member		
	A	*B*	*C*
1	0.3	0.4	0.3
2	.5	0	.5
3	0	.9	.1
4	.9	.1	0
5	1.0	0	0
6	0	.3	.7
7	.3	.2	.5
8	.4	.3	.3
9	.2	.5	.3
10	.4	0	.6

vectors in figure 1*A*; a possible problem with this sort of straightforward vector representation is that the vectors cluster near the reference axis representing the variable (SiO_2 in this case) with the highest mean. That is, the configuration of the vector cluster may be controlled dominantly by the variable means and standard deviations. The result is that the vector analysis of most igneous-rock data will be dominated by SiO_2 and, to a lesser extent, by Al_2O_3. Relatively minor constituents such as iron, magnesium, calcium, and especially trace elements will exert little influence on the vector configuration, even though these constituents can be more diagnostic of igneous processes than SiO_2 and Al_2O_3. Manson and Imbrie (1964) recognized this difficulty and scaled all variables to range from zero to unity, and Klovan and Imbrie (1971) equipped their factor analysis computer program (CABFAC) with the facility to scale the original data to either proportions of the variable range (that is, to range from zero to unity) or proportions of the maximum value for each variable. The mathematical effect of these transformations is to give each compositional variable approximately the same mean and standard deviation and to allow the sample vectors to occupy the full dimensions of the space in which they are represented mathematically (fig. 1*B*). The important consequence is that minor constituents can be just as influential on the factor analysis outcome as major ones, and, therefore, just as diagnostic of processes of rock origin.

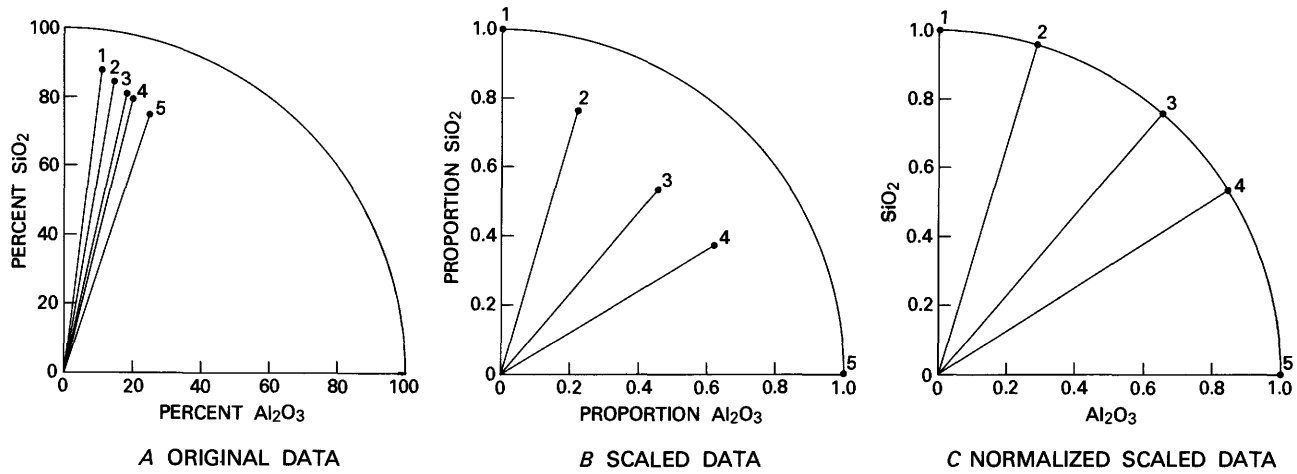

FIGURE 1.—Vector diagrams representing three forms of the same data for five hypothetical rock samples.

Scaling of the jth variable (oxide) to proportions of the total range is according to:

$$x_j' = \frac{x_j - x\min_j}{x\max_j - x\min_j}$$

where x_j is the original data value (generally the weight percent of an oxide), $x\max_j$ and $x\min_j$ are, respectively, the maximum and minimum values for the jth variable, and x_j' is the scaled data value. Scaling to proportions of the maximum is performed simply by dividing each value of x_j by $x\max_j$.

In the treatment of major-element (oxide) data in petrology, transformation of the variables by scaling is generally helpful, although not in all cases. The decision to scale or not to scale this type of data should be based on experimentation. If the data are not scaled, the mixing proportions derived from the extended Q-mode method for a given set of end-member compositions are the same as those derived by the least-squares method of Bryan, Finger, and Chayes (1969).

Whether the variables are scaled or not, a final data transformation is used in Q-mode factor analysis to adjust all vectors to unit length (that is, row-normalize). This is done by dividing each original or scaled analysis through by the square root of the sum of squares. This is for mathematical convenience and has no effect on the positions of the vectors relative to each other (fig. 1*C*).

VECTOR CONFIGURATIONS

Although the vector systems represented in figure 1 are based on only two compositional variables (SiO_2 and Al_2O_3), the same procedures can be used in mathematical, rather than graphical, form no matter how many variables are treated. Other mathematical procedures can be used to determine the extent to which the vectors occupy various dimensions of the multidimensional space; the total number of dimensions equals the number of oxides being used in the analysis. The procedures are principally those of eigenvalue analysis. The eigenvalues[1] for a vector system are measures of the variability within the system that occurs within the major dimension of the vector cluster, the second greatest dimension, the third, and so forth. Thus, if all but two of the eigenvalues are zero, the vector system occupies two dimensions only (that is, the vectors all lie within the same plane), even though the analytical data were mathematically represented in a number of dimensions equal to the number of oxide variables. Similarly, if all but three of the eigenvalues are zero, the vectors occupy a three-dimensional subset of the original multivariate space.

The eigenvalues for the vector systems representing the data in tables 1 and 2 are given below. They are listed in order of decreasing magnitude:

Eigenvalue No.	Eigenvalues	
	Table 1	Table 2
1	7.68	7.52
2	1.17	1.57
3	.62	.91
4	.24	0
5	.17	0
6	.10	0
7	.02	0
Total	10.00	10.00

In most applications of eigenvalue analysis, it happens that most of the eigenvalues are nonzero, but that some are small relative to others. Thus, if the first m eigenvalues are distinctly large relative to the others,

[1]All eigenvalues referred to in this report were computed for the minor product of the scaled (zero to one) and row-normalized data matrix and its transpose. Computer programs for the derivation of eigenvalues are available at most computer installations.

the vectors are known to cluster about an m-dimensional subspace rather than lie precisely within it. Each of the vectors can then be projected [2] into the subspace. The projected vectors then become somewhat less than unity in length, and because they are in different positions, represent compositions somewhat different from the original compositions of the corresponding samples. However, if all but the first m eigenvalues are close to zero, and the amount of projection, therefore, is small, the projected vectors remain close to unity in length and the modified (recomputed) compositions are not greatly different from the original sample compositions. The square of the length of a projected vector is referred to as the vector communality (h^2), and is the conventional measure of the degree to which a specific composition corresponds to the compositional series represented by a vector system.

If the first m eigenvalues are distinctly large relative to the others, the projection of the vectors into m-dimensional space is done on the presumption that m end members have been dominant in controlling the compositional variation within the rock body represented by the samples. Assuming that the laboratory errors are uncorrelated among the various constituents determined, there is no other circumstance that could cause the m eigenvalues to be large relative to the others. Those who may doubt the practical value of eigenvalues can explore their usefulness easily by means of simulation. Simply form some data by mathematical mixing of any given end-member compositions and then determine the eigenvalues of the minor product of the row-normalized data matrix and its transpose. It will be observed, for example, that when a number of end members equal to or greater than the number of oxides (M) are mixed in any proportions that are not perfectly correlated, the eigenvalues tend to be all nonzero. If only m end members ($m<M$) are mixed, only m eigenvalues will be nonzero.

The interpretation of vector systems representing rock compositions can be explained by reference to figure 2. Figure 2 is a stereogram constructed by projecting vectors from an upper hemisphere vertically onto the plane of the diagram. (The same projection was used for constructing other stereograms given in this report. See figures 9, 10, and 12.) Nine hypothetical sample compositions, ranging from basalt (vector B) to rhyolite (vector R), are represented by vectors that all lie within the same plane (XR). The first two eigenvalues describing the configuration of the vector system are positive and the remainder are zero. The only likely natural process that would lead to a vector system such as this—with all sample vectors in the same plane—is one involving the mixing of two, and only two, end members. Moreover, the two end members must have had compositions that can be represented as vectors in the same plane (XR). For example, the composition of sample 2 (fig. 2) can be reproduced by mixing 0.5 parts of composition B and 0.5 parts of composition R, and the composition of sample 6 can be reproduced by mixing 0.2 parts of composition B and 0.8 parts of composition R. Alternatively, the composition of sample 2 can be reproduced by separating 1.1702 parts of composition X from 2.1702 parts of composition B, and the composition of sample 6 can be reproduced by separating 1.8723 parts of composition X from 2.8723 parts of composition B. In contrast, a sample formed by the mixing of composition B with some composition represented by a vector

[2]The sample vectors are projected by rotation of the first m principal component axes according to the varimax criterion of Kaiser (1958).

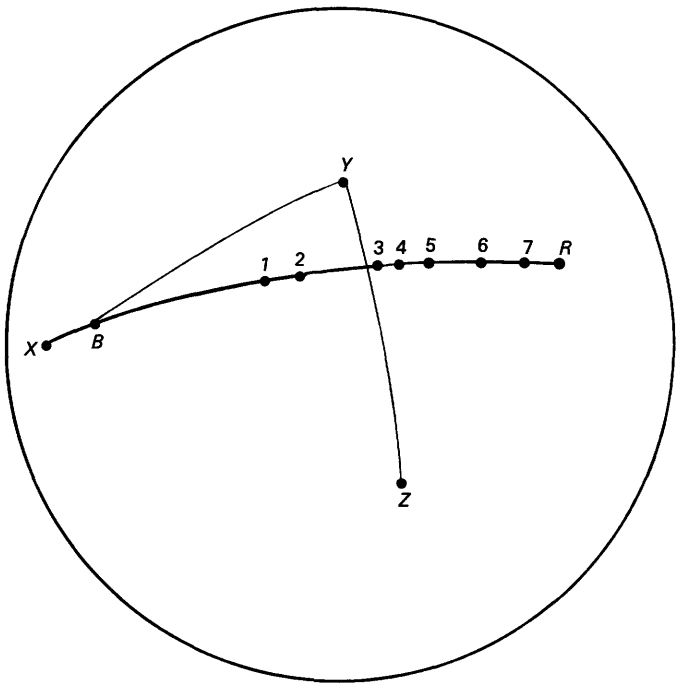

FIGURE 2.—Stereogram showing a configuration of vectors representing the compositions of some hypothetical samples.

	Compositions represented by vectors, in weight percent					
Oxide	*B*	1	2	3	4	5
SiO_2	51.25	61.64	62.79	65.56	66.25	67.41
Al_2O_3 ..	16.40	15.15	15.01	14.67	14.59	14.45
"FeO" ..	11.71	7.49	7.02	5.89	5.61	5.14
MgO ...	6.45	3.72	3.42	2.69	2.51	2.21
CaO	9.35	5.70	5.30	4.33	4.08	3.68
Na_2O ...	3.25	3.32	3.33	3.35	3.35	3.36
K_2O	1.59	2.98	3.13	3.50	3.60	3.75

Oxide	6	7	*R*	*X*	*Y*	*Z*
SiO_2	69.72	72.02	74.33	41.39	62.72	68.47
Al_2O_3 ..	14.17	13.89	13.62	17.59	15.27	13.97
"FeO" ..	4.21	3.27	2.33	15.72	6.87	4.97
MgO ...	1.60	.99	..39	9.03	3.23	2.22
CaO	2.87	2.06	1.25	12.81	5.12	3.59
Na_2O ...	3.38	3.40	3.41	3.18	3.43	3.23
K_2O	4.06	4.37	4.68	.27	3.36	3.56

outside the plane *XR*, say vector *Y*, would have a composition represented by a vector in the plane *BY*.

It is mathematically possible to generate the compositional series represented by vectors in the plane *XR* by mixing more than two compositions represented by vectors outside of the plane *XR*, but the process, in effect, would be the same as mixing only two end members. For example, samples 1 and 2 in figure 2 could result from the mixing, in positive proportions, of compositions *B*, *Y*, and *Z*, and samples 3 through 7 could result from the separation of composition *B* from a mixture of compositions *Y* and *Z*. However, in each case, the proportion of composition Y would have to be exactly 1.417 times greater than the proportion of composition *Z*—no more and no less. The result would be a composition that could be represented by a vector in the plane *XR*, at the intersection of the planes *XR* and *YZ*. Thus, the two end members, *Y* and *Z*, effectively would be only one.

The same principles of vector addition and subtraction can be extended to situations where the sample vectors fall not on a plane, but within a factor space of three dimensions, four dimensions, or more.

FACTOR-VARIANCE DIAGRAMS

Although the eigenvalues serve to describe important aspects of the vector configurations, they give little information about the differences between the compositions represented by projected vectors and the actual compositions of the samples that the vectors represented before projection. If these differences are larger than can be attributed to analytical errors and to minor petrologic processes, the number of end members for the model, *m*, will have to increased. If the differences are acceptable, however, the projected vector configuration may provide a basis for developing a petrologic model, or for testing a previously developed model. The extended *Q*-mode procedures (Miesch, 1976a, 1976b) always lead to matrices of recomputed data (represented by the projected vectors) that have column (oxide) means essentially the same as those of the original data. The correlations between corresponding columns, from one matrix to the other, however, range from near zero to unity, depending on the degree of compositional modification that occurred with projection. The square of each correlation, r^2_j, is a measure of the maximum proportion of the variance in each oxide that can be accounted for by a model with *m* end members.

Factor-variance diagrams are constructed by plotting r^2_j for each oxide against the number of end members in the model, and show the maximum proportion of the total variance in each oxide that can be accounted for by mixing *m* end members. Factor-variance diagrams were given previously (Miesch, 1976b) for four suites of samples from (1) a rhyolite-basalt complex in Yellowstone National Park, Wyoming (Fenner, 1938), (2) a granitoid intrusive in eastern Nevada (Lee and Van Loenen, 1971), (3) lavas and pumices from the 1959 summit eruption at Kilauea, Hawaii (Murata and Richter, 1966), and (4) the layered series of the Skaergaard intrusion, Greenland (Wager and Brown, 1968). Another factor-variance diagram was given previously for a single pluton of the southern California batholith (Miesch and Morton, 1977). The implications of these diagrams with respect to the origins of the rocks they represent are discussed in the cited references.

Factor-variance diagrams for the hypothetical-data matrices in tables 1 and 2 are given in figure 3. The differences between the diagrams clearly indicate the difference in compositional structure referred to previously. Figure 3 shows that seven end members are required to account for all of the variance in all the constituents for the data in table 1, whereas all of the variance in each of the constituents for the data in table 2 can be explained by mixing only three end members.

Factor-variance diagrams representing two real igneous bodies are given in figures 4 and 5. The diagram in figure 4 pertains to the Pikes Peak batholith in Colorado; the data used in constructing it are from Barker and others (1975, tables I and IV), and consist of measurements for 7 oxides in 41 samples, principally of quartz syenites, fayalite granites, and fayalite-free granites. The diagram shows that two- and three-end-member models would fail to account for much of the compositional variability in the batholith, and that even a four-end-member model would leave 20 percent of the variability in K_2O and MgO unexplained. The compositoinal structure in the batholith, therefore, appears to be complex. This is in accord with the complex model of origin that Barker and others have developed on conventional petrologic and geochemical grounds. The model includes the incorporation of lower and intermediate crusts into, respectively, basaltic and syenitic magmas, with the crystallization and separation of phases such as olivine, clinopyroxene, and feldspars. Also, both of the crustal materials and each of the separated phases could have been of variable composition.

The factor-variance diagram in figure 5 pertains to the McCartys Basalt (Holocene) in northwestern New Mexico. The data used are from Carden and Laughlin (1974) and consist of measurements on 7 oxides in 37 samples. The diagram indicates that two- to four-end-member models would be inadequate to account for any appreciable proportion of the compositional variance in the flow. The compositional structure in the flow is complex. This is in accord with the model of Carden and Laughlin, which involves crystal fractiona-

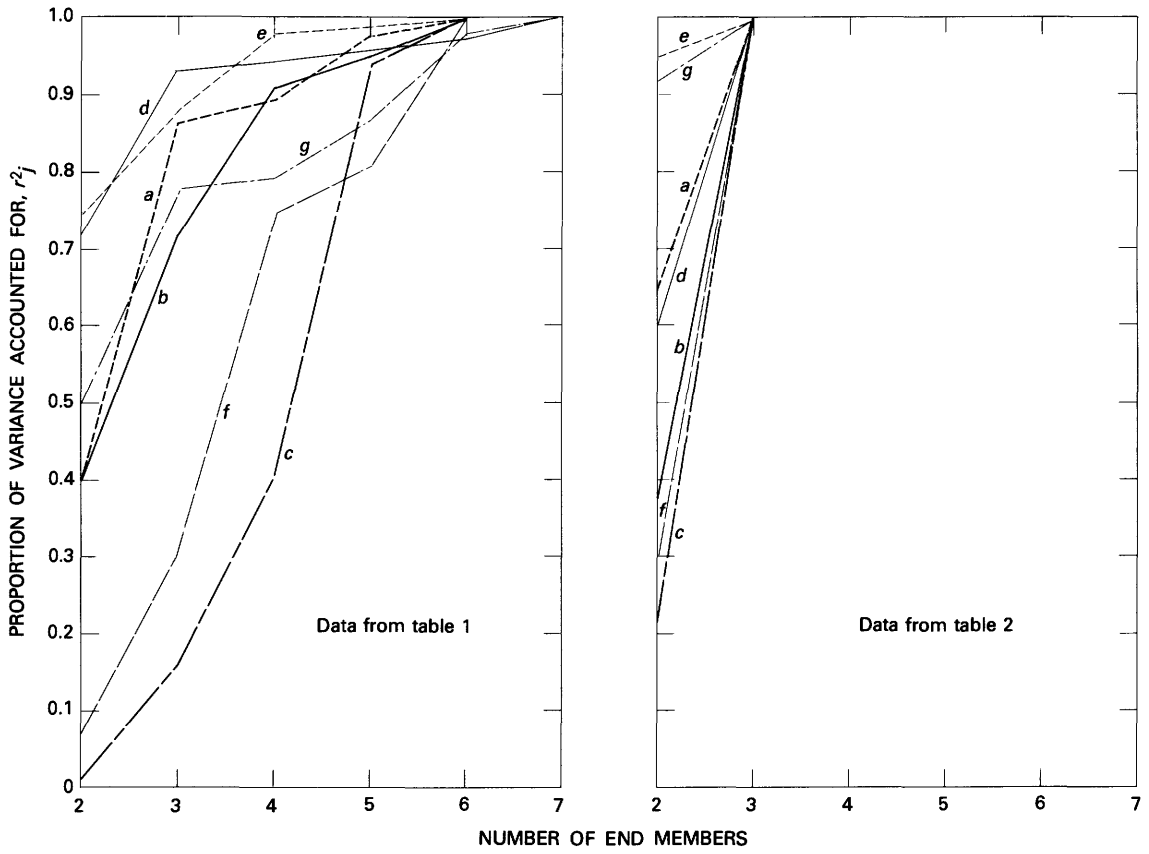

FIGURE 3.—Factor-variance diagrams for the data for constituents a–g in tables 1 and 2.

tion of plagioclase, olivine, and pyroxene, all of variable composition, in addition to several accessory minerals.

COMPOSITIONAL STRUCTURES IN THE SIERRA NEVADA AND ALASKA-ALEUTIAN RANGE BATHOLITHS

The geology of the Sierra Nevada batholith in eastern California (fig. 6) has been summarized by Bateman and others (1963). The batholith consists primarily of quartz-bearing granitic rocks that range in composition from quartz diorite to alaskite. The rocks occur as discrete plutons, and groups of plutons form sequences. Plutons within a sequence tend to be spatially continuous with each other and of about the same age. Definitions of the sequences within the batholith were by Bateman and Dodge (1970), although they apply the less formal term "rocks" in place of the term "sequence" wherever the age relations are not entirely certain. The same authors retain a previously assigned name, "Toulumne intrusive series," for one group of plutons that has the characteristics of a sequence.

The chemical data on the Sierra Nevada batholith pertain to 228 samples collected from a large number of plutons in the central part by Paul C. Bateman and his colleagues. About one-half of the samples are from six previously defined sequences: White Mountains rocks, Palisade Crest sequence, Scheelite sequence, Toulumne intrusive series, Yosemite rocks (called Yosemite intrusive series by Wright, 1975), and the Shaver sequence (Bateman and Dodge, 1970, fig. 2). The area represented is about the same as that reported on by Bateman and Dodge (1970) in their examination of chemical variations across the batholith. Seven major oxides (SiO_2, Al_2O_3, 'FeO'[3], MgO, CaO, Na_2O, and K_2O), recalculated to sum to 100 percent, are represented in the data. These oxides were selected because they are essential in the principal rock-forming minerals.

The eigenvalues describing the dimensionality of the vector system representing the data, before projection, are 198.3, 24.3, 2.8, 1.4, 0.7, 0.4, and 0.2. Thus, the vectors cluster about a two-dimensional space, even though they were mathematically represented in 7 dimensions. The factor-variance diagram in figure 7, however, indicates that the compositions represented

[3]As used in this report, 'FeO' equals $FeO+0.9Fe_2O_3$, and thus represents total iron.

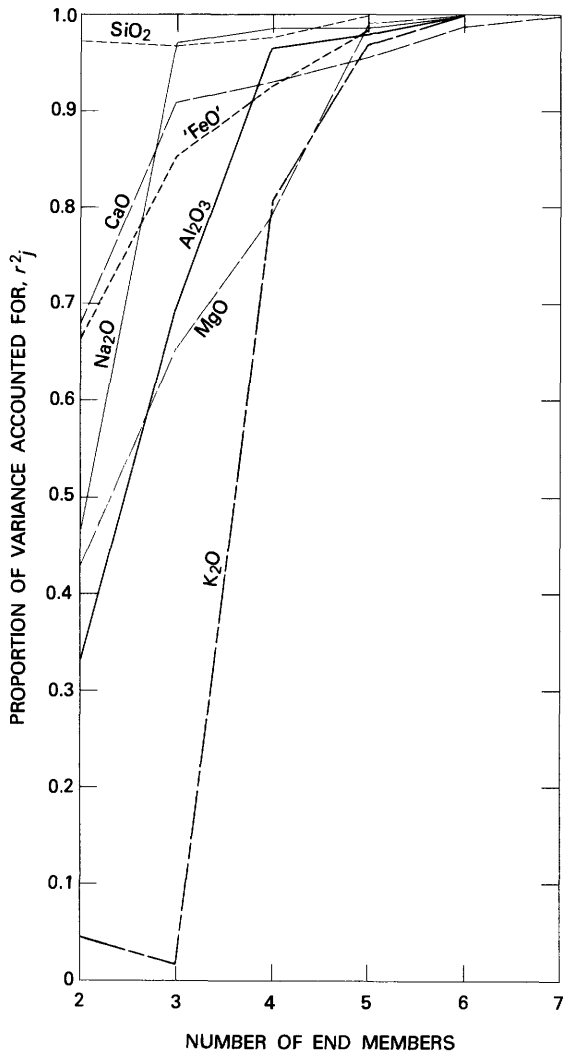

FIGURE 4.—Factor-variance diagram for the Pikes Peak batholith, Colorado.

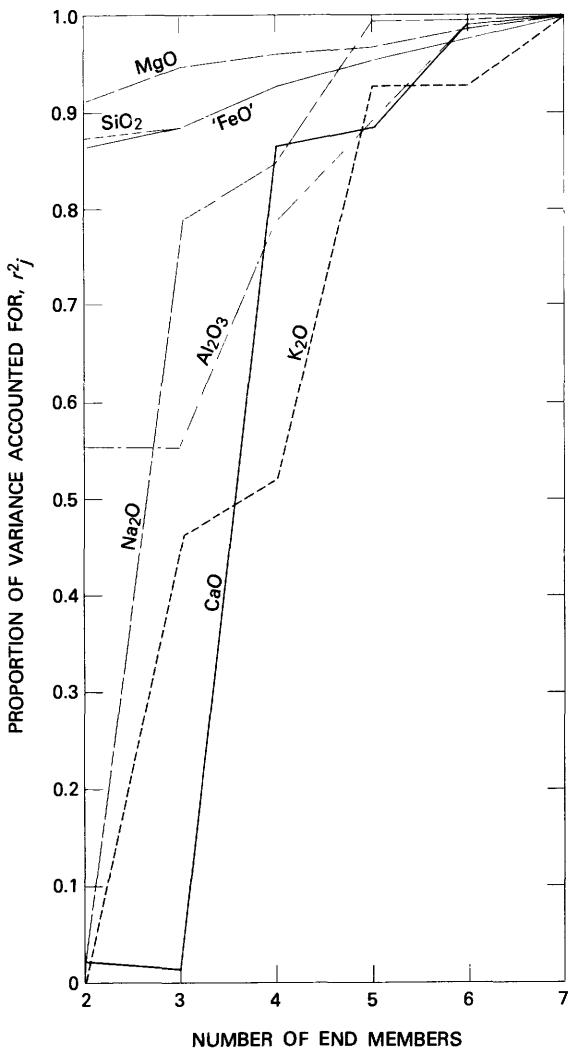

FIGURE 5.—Factor-variance diagram for the McCartys Basalt (Holocene), New Mexico.

by the vectors after they have been projected into a plane are greatly different from the original compositions with respect to K_2O, Al_2O_3, and especially Na_2O. But, the diagram also shows that if the vectors are projected into a three-dimensional space, rather than into a plane, all of the recomputed compositions are at least moderately close to the observed compositions of the samples. Three-end-member models can account for 77 to 97 percent of the variance in each oxide. If the vectors are projected into four-dimensional space, the situation is improved still further. Four-end-member models can account for 90 to 99.9 percent of the variance in each oxide.

The eigenvalues and the factor-variance diagram indicate, therefore, that the compositional structure of the Sierra Nevada batholith is fairly simple. Three end members can account for most of the variation in the data and an additional end member improves this substantially. The remaining variation can be attributed to minor geochemical processes and to analytical variance. Some of it may also be attributed to small compositional variations within each of four principal end members.

The Alaska-Aleutian Range batholith (fig. 6), like the Sierra Nevada batholith, is composed of discrete plutons that can be assigned to sequences (Reed and Lanphere, 1969, 1973). The rocks range in composition mostly from diorite to granite. The analytical data used in the vector (*Q*-mode factor) analysis are from 158 samples, and consist of measurements of the same seven oxides used in the Sierra Nevada analysis. Data for 79 of these samples are given in Reed and Lanphere (1974); the remaining 79 samples were collected more recently, chiefly from the northern part of the batholith, and were analyzed for this study. These rocks are classified into 9 groups according to their age

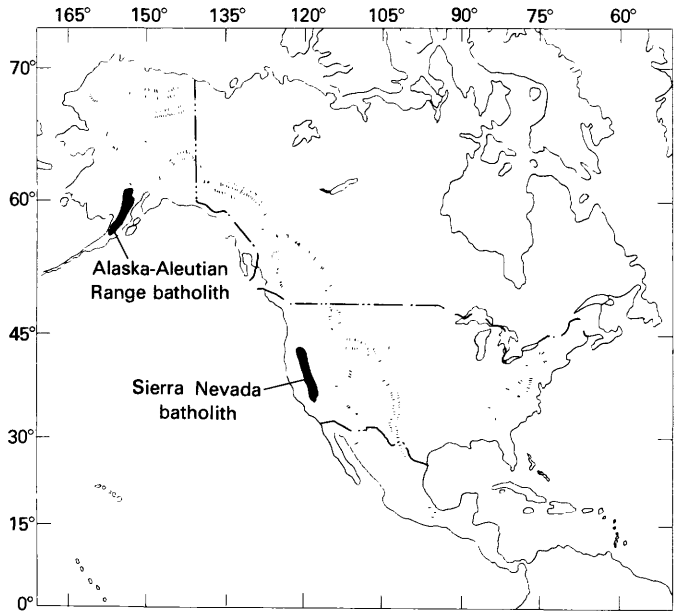

FIGURE 6.—Index map of the northeastern circumpacific region, the Alaska-Aleutian Range batholith and the Sierra Nevada batholith.

and chemical characteristics (Reed and Lanphere, 1973). Of the 79 additional samples, 53 are from the same groups of rocks discussed by Reed and Lanphere (1974) and 26 are from the granodiorite of Mount Estelle, the Hartman sequence, and the Yentna sequence. (See Reed and Lanphere, 1973, fig. 2.) The oldest group consists of samples from plutonic rocks of Jurassic age. Seven groups are of samples from rocks of Late Cretaceous–early Tertiary age. The final group is from the Merrill Pass sequence of middle Tertiary age. The rocks of Jurassic age range mostly from diorite to granodiorite, whereas quartz monzonites and granites make up much of the younger groups.

The eigenvalues for the vector system constructed in seven dimensions on the basis of the seven oxides are 129.2, 22.0, 5.4, 0.7, 0.4, 0.2, and 0.1. Like those for the Sierra Nevada rocks, these values indicate that the vector system occurs principally in two or three dimensions. The factor-variance diagram (fig. 8), however, shows that models with three end members are required to account for all of the seven oxides. Three-end-member models can account for 92 to 98 percent of the variance in each oxide. Unlike the factor-variance diagram for the Sierra Nevada batholith, figure 8 shows that a fourth end member would do little to improve the model for the Alaska-Aleutian Range batholith.

The average compositions of both batholiths, estimated from the data referred to, are given in table 5 along with the amount of absolute variance in each batholith that can be accounted for, and the amount

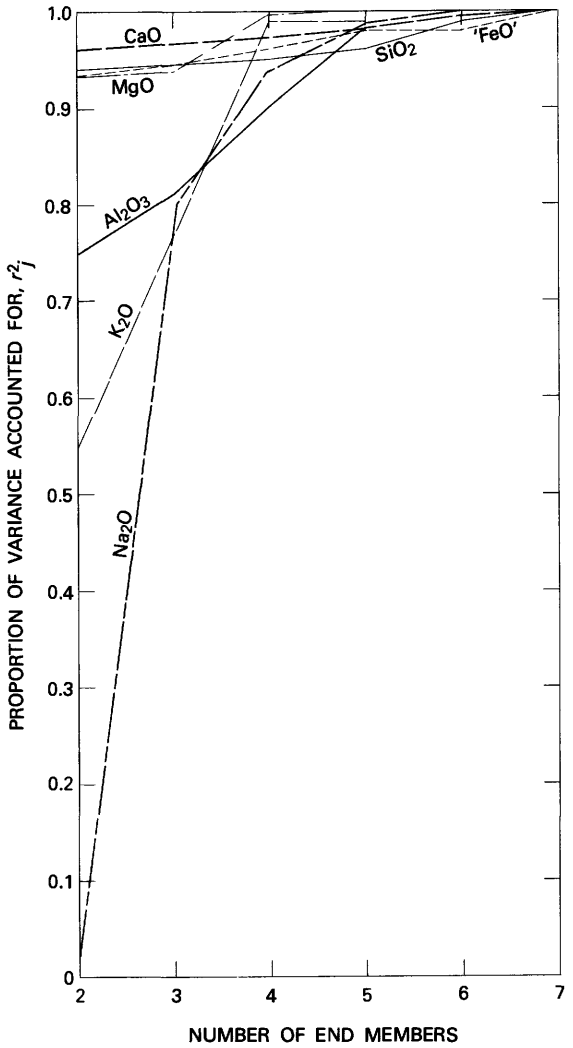

FIGURE 7.—Factor-variance diagram for the Sierra Nevada batholith.

that cannot be accounted for, by mixing models with the indicated number of end members. The average compositions of groups of plutons within each batholith are given in tables 6 and 7.

As comparison of figures 7 and 8 shows, the compositional structure in the Alaska-Aleutian Range batholith is similar to that in the Sierra Nevada batholith, although probably even less complex. With the exception of Na_2O, more than half of the variance in each oxide can be accounted for by only two end members for each batholith (figs. 7 and 8). Three end members can account for more than 90 percent of the variances in all oxides in the Alaska-Aleutian Range batholith and for more than three-fourths of the variances in all oxides in the Sierra Nevada batholith; a fourth end member increases the variances accounted for in the Sierra Nevada batholith to more than 90 percent.

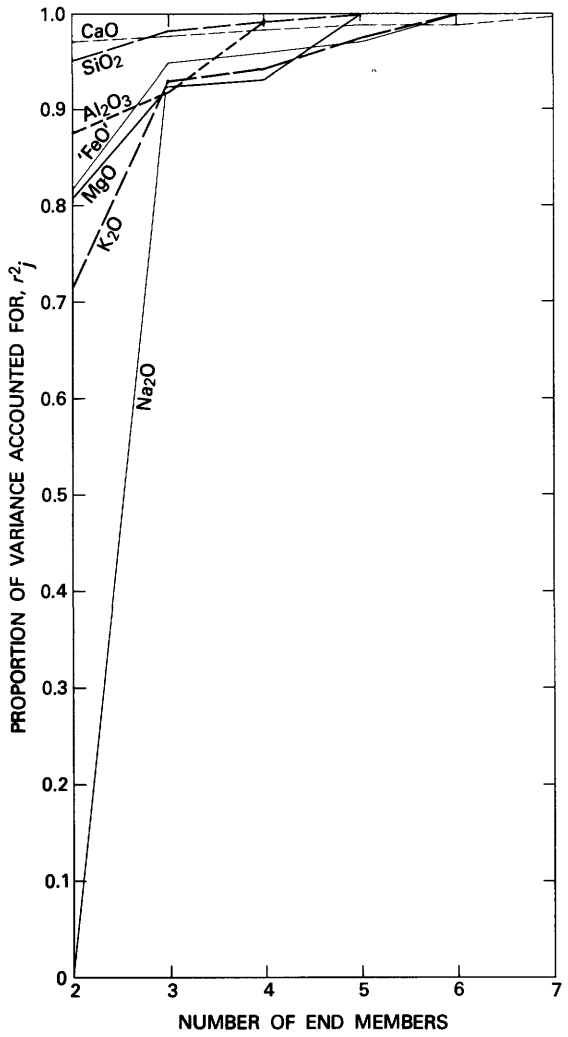

FIGURE 8.—Factor-variance diagram for the Alaska-Aleutian Range batholith.

The simplicity of the compositional structures in both batholiths, compared to those determined for some other igneous bodies, suggests that the major features of their compositional variation in both space and time can be attributed to only a few dominant geologic processes. For example, these variations could arise from a single, homogeneous magma or melt if only two mineral assemblages were separated from it by fractional crystallization and settling, or if one mineral assemblage that varied in composition within a two-end-member system were separated out. Alternatively, the processes may have consisted of the mixing of three magmas or of a magma and two other materials, possibly by assimilation of crustal or subcrustal materials. The important point is that a process involving three dominant end members can explain major parts of the observed compositional variation in both batholiths. The remaining variation can be attributed to processes or factors that were of relatively minor importance in causing compositional variation. These minor factors include small compositional variations in each of the end members, minor petrologic processes, and variation caused by analytical procedures.

A fourth end member is required in the model for the Sierra Nevada batholith in order to account for about the same proportions of the total variances that are accounted for by three-end-member models for the Alaska-Aleutian Range batholith. However, the fourth end-member should be one that serves only to refine a basic three-end-member model.

SPECULATION ON END-MEMBER COMPOSITIONS

The relatively simple compositional structures of the Sierra Nevada and Alaska-Aleutian Range batholiths suggest that the processes of their formation were not highly complex, at least not complex in terms of the number of independent phases involved, and this leads us to speculate what these end members might have been.

The only end-member compositions that will serve to reproduce the original data to the degrees indicated by

TABLE 5.—*Average compositions of the Sierra Nevada and Alaska-Aleutian Range batholiths and absolute variances accounted for and not accounted for by various mixing models*

	Sierra Nevada batholith						Alaska-Aleutian Range batholith			
			Three-end-member model		Four-end-member model				Three-end-member model	
Constituent	Average concentration (percent)	Total variance	Variance accounted for	Variance not accounted for	Variance accounted for	Variance not accounted for	Average concentration (percent)	Total variance	Variance accounted for	Variance not accounted for
SiO_2	69.49	20.5363	19.2936	1.2427	20.5065	0.0298	68.60	39.9159	39.1547	0.7612
Al_2O_3	15.51	1.7182	1.3871	.3311	1.5512	.1670	15.89	3.4611	3.1885	.2726
'FeO'	3.33	2.8348	2.6871	.1477	2.7092	.1256	3.62	4.4610	4.2504	.2106
MgO	1.25	.7762	.7389	.0373	.7438	.0324	1.53	2.1159	1.9757	.1402
CaO	3.16	2.4649	2.3812	.0837	2.3964	.0685	3.44	5.2624	5.1472	.1152
Na_2O	3.49	.1936	.1551	.0385	.1817	.0119	3.87	.4575	.4230	.0345
K_2O	3.76	.8610	.6601	.2009	.8545	.0065	3.05	1.7363	1.6084	.1279

TABLE 6.—*Average compositions of groups of plutons in the Sierra Nevada batholith*

[All analyses were recomputed to 100 percent before computation of averages]

Group of plutons	Number of samples	SiO_2	Al_2O_3	'FeO'	MgO	CaO	Na_2O	K_2O
White Mountains rocks	21	66.84	16.40	3.84	1.55	3.22	3.61	4.53
Palisade Crest sequence	19	66.62	15.85	4.31	1.70	3.96	3.48	4.09
Scheelite sequence	23	72.30	14.32	2.50	.81	2.47	3.10	4.50
Toulumne intrusive series	7	69.72	15.58	2.97	.82	3.39	3.94	3.57
Yosemite rocks	7	74.01	14.61	1.57	.42	2.07	3.67	3.65
Shaver sequence	36	70.71	15.20	3.21	1.05	2.87	3.27	3.68
All other plutons	115	69.22	15.68	3.41	1.36	3.30	3.58	3.46
All plutons	228	69.49	15.51	3.33	1.25	3.16	3.49	3.76

TABLE 7.—*Average compositions of groups of plutons in the Alaska-Aleutian Range batholith*

[All analyses were recomputed to 100 percent before computation of averages]

Group of plutons	Number of samples	SiO_2	Al_2O_3	'FeO'	MgO	CaO	Na_2O	K_2O
Merrill Pass sequence	29	75.10	13.78	1.76	0.38	1.39	3.88	3.72
Quartz monzonite of Tired Pup	14	73.41	14.24	2.55	.39	1.44	3.31	4.67
Crystal Creek sequence	22	74.08	14.24	1.99	.31	1.24	3.94	4.19
Hartman sequence	5	66.79	15.76	4.32	2.64	4.32	3.01	3.25
Granodiorite of Mount Estelle	13	66.77	16.28	4.32	2.01	3.61	3.21	3.81
Yentna sequence	8	64.31	16.50	4.91	2.89	4.25	3.21	3.93
Summit Lake rocks	35	64.73	17.66	4.36	2.01	5.05	4.44	1.75
Undivided plutonic rocks	3	70.38	15.19	2.93	1.76	2.99	3.22	3.52
Plutonic rocks of Jurassic age	29	62.41	17.66	5.63	2.76	5.81	4.09	1.63
All plutons	158	68.60	15.89	3.62	1.53	3.44	3.87	3.05

the factor-variance diagrams (figs. 7 and 8) are those that can be represented by vectors in the corresponding vector spaces. These vectors then can be used as reference vectors for describing the compositional systems. Mathematically satisfactory reference vectors, representing end-member compositions, can be found for the three- and four-end-member models by determining the compositions represented by hypothetical vectors throughout the three- and four-dimensional vector spaces. This must be done at increments inasmuch as the number of hypothetical vectors is infinite. Reference vectors may also be found by representing selected compositions as vectors in the three- and four-dimensional systems of sample vectors and determining the vector communalities. If the compositions can be represented in this manner (that is, if the vector communalities are close to unity), they can be accepted as mathematically suitable end members for the model. After plausible end-member compositions have been identified in either manner, it remains only to determine the required mixing proportions. If these proportions are geologically unreasonable or unlikely, another set of end-member compositions can be tried until the end-member compositions and the mixing proportions are not incompatible with whatever is known about the rock body and petrologic processes in general. It will be apparent from this that the procedures lead to a petrologic model only, and that a unique solution to the origin of the rock body, by this means, is impossible. The computer programs used in the modeling procedure are referred to in the appendix.

Representation of selected compositions as vectors in the three- and four-dimensional vector systems for the two batholiths indicate that none of the end members could have had the compositions of common hornblende, biotite, quartz, or any feldspar, even though it seems obvious from field observations that these minerals were involved in fractional crystallization of the magmas. Moreover, none of the end members could have had the composition of any pyroxene or olivine. Consequently, it is likely that the end-member compositions were those of mineral mixtures, either clusters or assemblages of minerals or compositionally equivalent liquid phases.

If a major part of the compositional variability in each batholith is the result of the separation or redistribution of mineral assemblages, the observed compositional structures place constraints on the nature of the compositional variations within these assemblages. At least one of the end members for each batholith must be reserved to represent the parent

magma or the magma-source material. The compositional variation in the mineral assemblages, therefore, must be of a kind that can be described largely in terms of a two-component system, inasmuch as only three end members controlled a major part of the variation in each batholith. There is no doubt that the mineral assemblages varied in composition in both space and time.

A model consisting of a parent magma or a magma-source material from which mineral assemblages separated or were redistributed is not the only one that might be accepted as geologically plausible. However, this type of model is relatively simple compared with other three-end-member models that might be proposed, and it seems reasonable to consider the most simple model first. Also, it is apparent from field observations that important amounts of compositional variation within and among plutons were caused by the redistribution of crystalline phases.

If the possibility that the determined compositional structures of the batholiths arose by chance is discounted, and if the end members contributng to the batholiths' formation are accepted as a magma, or magma-source material, and mineral assemblages of varying composition, other processes must be excluded as quantitatively important causes of variation within the batholiths. These other processes include magma mixing and assimilation of crustal and subcrustal materials. This may be the most important consequence of the determination that both batholiths have simple compositional structures.

Furthermore, if we accept that the compositional structures of the batholiths resulted from the separation of mineral assemblages from a magma or magma-source material, then there is little room in the model for compositional variations among the magmas or within the magma-source material. Bateman and Dodge (1970) and Reed and Lanphere (1974) showed that the K_2O contents of the granitic rocks vary across the batholiths, and they interpreted the variation to reflect compositional variations in the magma-source materials. This interpretation still seems valid although it should be recognized that only a small part of the variance in K_2O, and even less of the variance in most of the other oxides, is associated with the variance across the batholith. Reed and Lanphere (1974, p. 351) gave the correlation coefficient for K_2O content and distance across the Alaska-Aleutian Range batholith as -0.53. The square of this value (0.28) gives the proportion of the total variance in K_2O associated with distance. Clearly, other factors were far more important in controlling the compositions of the granitic rocks. Reed and Lanphere (1974) made the additional observation that trends in K_2O and other oxides within groups of plutons are commonly opposite to those observed across the entire Alaska-Aleutian Range batholith. It will be shown that compositional variations among the magmas or magma-source materials can be represented in a four-end-member model for the Sierra Nevada batholith, but this model is only a refinement of a three-end-member model that accounts for most of the compositional variation.

Stereograms of the three-dimensional vector systems for the two batholiths are given in figures 9 and 10. All vectors have been restored to unit length after projection into three-dimensional space, and are shown as points that have been projected vertically from an upper hemisphere. The natures of the compositional systems represented by the diagrams are shown by the compositions of selected hypothetical vectors in tables 8 and 9. Any hypothetical vectors that might occur outside the areas enclosed by dotted lines on figures 9 and 10 would represent compositions that are partly negative; only vectors within or near these areas need be considered.

A search for the compositions of mineral assemblages that might have separated from or been redistributed in the magmas was made by examination of the compositional system formed by hornblende, albite, anorthite, and magnetite. It is expected that the earliest formed assemblages, at least, would have had total compositions within the range of compositions of these phases. The composition of hornblende was taken as the average composition of 22 hornblendes from the central part of the Sierra Nevada batholith (table 10). The hornblende data are from Dodge, Papike, and Mays (1968), who pointed out that the data may not be representative of hornblendes that precipitated early. However, experimentation with other hornblende compositions, including those given for "early" hornblendes by Nockolds and Mitchell (1946, table XIV, analyses 2–6), has led to results substantially the same as those described here. Ideal compositions were assumed for albite and anorthite, and the composition of magnetite in terms of the oxides being considered is 100 percent 'FeO'. The four-component compositional system was represented as a tetrahedron and examined throughout at increments of 2 weight percent; each of the 23,426 compositions was represented as a vector in the seven-dimensional vector space (based on the seven oxides) and then projected into the same three-dimensional space as the sample vectors (figs. 9 and 10). This procedure required less than one minute of computer processor time for each batholith.

Of the 23,426 compositions examined for the Sierra Nevada batholith, 385 could be represented by vectors

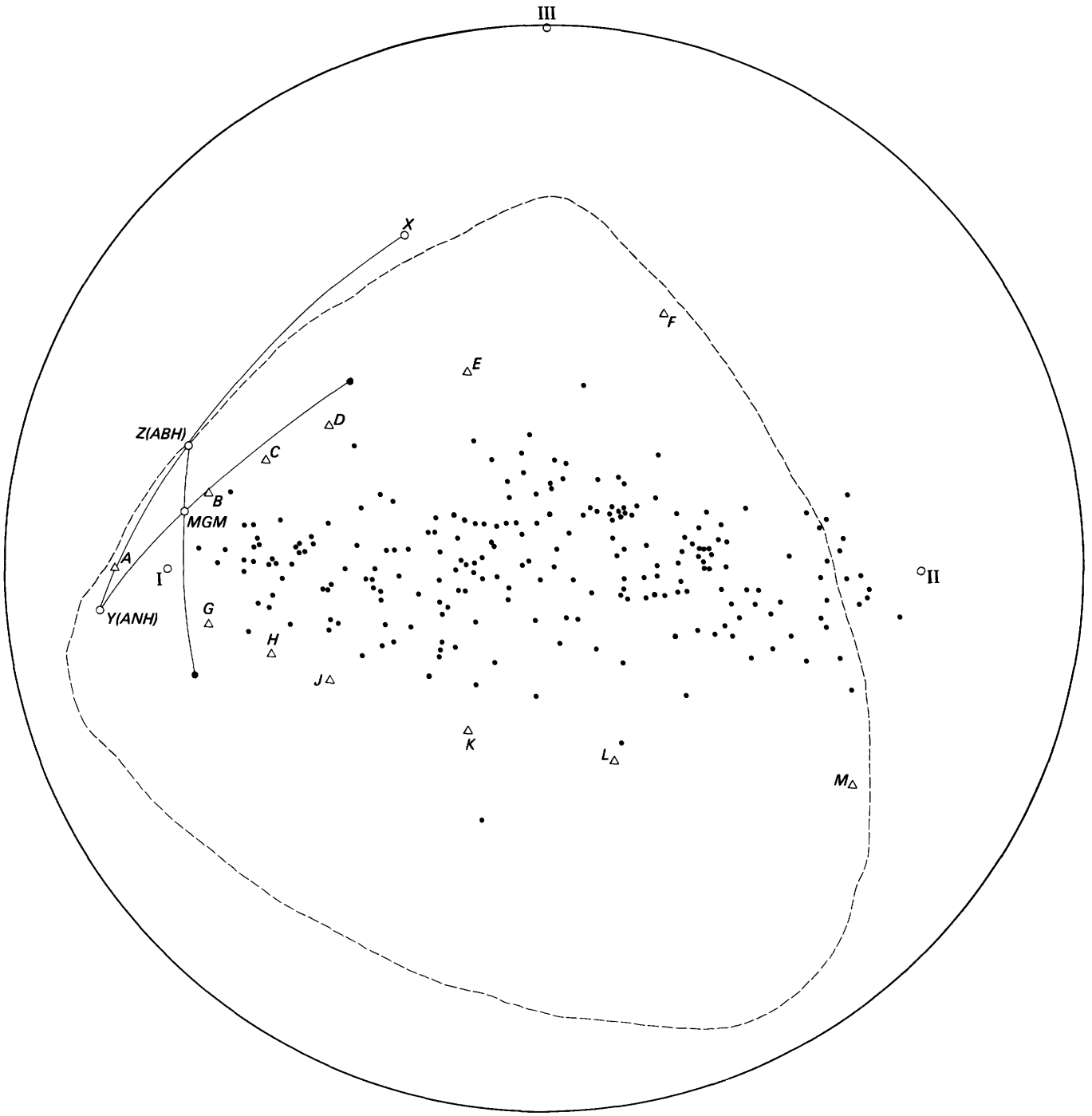

FIGURE 9.—Stereogram showing the three-dimensional vector system for the Sierra Nevada batholith. Dots represent 228 sample vectors. Open circles labeled I, II, and III represent the varimax reference axes. Lettered triangles represent hypothetical vectors referred to in text and in table 8. Dashed line represents boundary of area in which all vectors represent compositions that are entirely nonnegative.

with communalities greater than the arbitrary value of 0.98 in the three-dimensional vector system. The field containing these 385 compositions is indicated in figure 11*A*. The compositions represented by vectors with the highest communalities (as high as 0.9964) are represented by points that occur along the line *X*-*Y*. Thus, line *X*-*Y* is taken as the most likely trend of compositional variation within the mineral assemblages that separated from the Sierran magmas. Compositions along this trend are those within the system

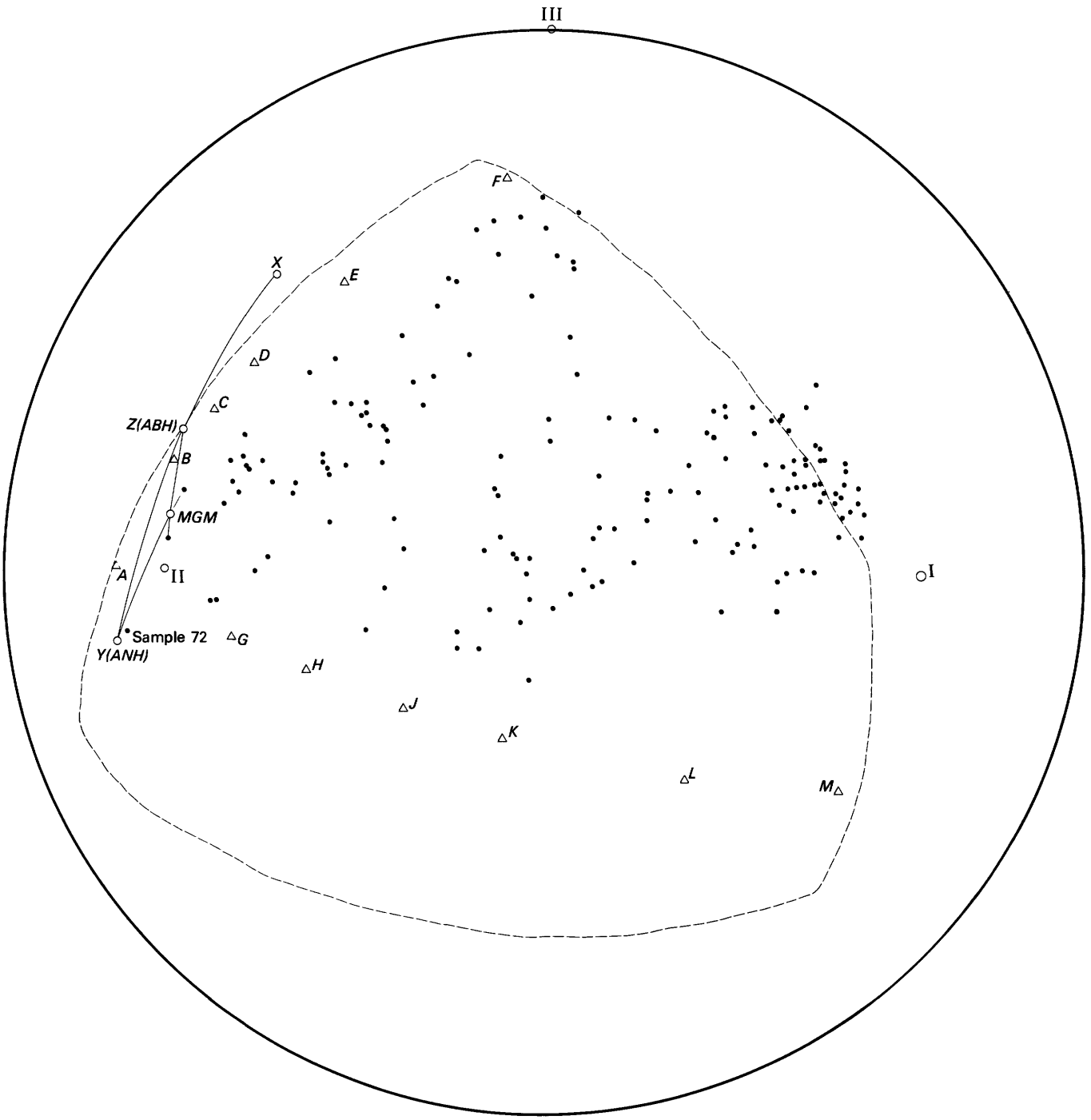

FIGURE 10.—Stereogram showing the three-dimensional vector system for the Alaska-Aleutian Range batholith. Dots represent 158 sample vectors. Open circles labeled I, II, and III represent the varimax reference axes. Lettered triangles represent hypothetical vectors referred to in text and in table 9. Dashed line represents boundary of area in which all vectors represent compositions that are entirely nonnegative.

albite-anorthite-hornblende-magnetite that are the most compatible with the compositional variations in the granites of the Sierra Nevada batholith.

Of the 23,426 compositions examined for the Alaska-Aleutian Range batholith, only 156 could be represented by vectors with communalities greater than 0.98 in the three-dimensional vector system. The trend of compositions represented by vectors with the highest communalities (as high as 0.9943) is shown by the line *X*-*Y* in figure 11*B*.

TABLE 8.—*Compositions (weight percent) represented by some hypothetical vectors in figure 9*

Oxide	Vector											
	A	*B*	*C*	*D*	*E*	*F*	*G*	*H*	*J*	*K*	*L*	*M*
SiO_2	46.43	57.41	60.84	63.47	67.69	72.77	58.81	62.12	64.67	68.54	71.70	77.41
Al_2O_3	21.48	19.16	18.47	17.92	17.04	15.97	17.87	16.90	16.15	15.02	14.10	12.43
'FeO'	11.85	7.49	6.19	5.16	3.51	1.52	7.47	6.30	5.40	4.03	2.92	.89
MgO	5.65	3.29	2.59	2.03	1.14	.06	3.47	2.88	2.43	1.75	1.20	.19
CaO	11.24	7.34	6.19	5.27	3.79	2.01	6.92	5.76	4.87	3.52	2.41	.42
Na_2O	2.95	3.93	4.22	4.46	4.83	5.27	2.68	2.61	2.55	2.47	2.40	2.27
K_2O	.41	1.24	1.49	1.69	2.01	2.40	2.79	3.43	3.92	4.67	5.28	6.38

TABLE 9.—*Compositions (weight percent) represented by some hypothetical vectors in figure 10*

Oxide	Vector											
	A	*B*	*C*	*D*	*E*	*F*	*G*	*H*	*J*	*K*	*L*	*M*
SiO_2	46.56	54.20	56.87	59.37	63.88	70.51	55.08	58.17	61.09	63.87	69.02	74.80
Al_2O_3	21.58	20.31	19.86	19.45	18.70	17.60	18.63	17.56	16.55	15.59	13.80	11.81
'FeO'	10.88	7.91	6.87	5.89	4.14	1.56	8.57	7.74	6.94	6.19	4.79	3.23
MgO	6.42	4.41	3.71	3.05	1.87	.12	4.87	4.30	3.77	3.26	2.32	1.26
CaO	11.22	8.76	7.90	7.10	5.65	3.52	7.95	6.77	5.64	4.58	2.61	.39
Na_2O	3.33	4.23	4.54	4.83	5.36	6.13	2.76	2.56	2.36	2.17	1.83	1.44
K_2O	.01	.19	.25	.31	.41	.56	2.14	2.92	3.65	4.34	5.63	7.07

TABLE 10.—*Average composition of hornblende from granitic rocks of the Sierra Nevada batholith*

[Data from Dodge, Papike, and Mays (1968) for 22 samples. All analyses were recalculated to sum to 100 before computation of average]

Constituent	Average (in percent)
SiO_2	48.89
Al_2O_3	8.14
'FeO'	16.42
MgO	12.55
CaO	12.26
Na_2O	1.06
K_2O	.68

Although the compositions along the trends *X-Y* in figure 11 are the compositions of best fit within the range of compositions examined, it is not expected that this range is all inclusive, because it is defined by ideal compositions for albite, anorthite, and magnetite and because the compositions of hornblendes can vary to some extent. Rather, the *X-Y* trends in figure 11 are taken as approximations of the most likely compositions of mineral assemblages that may have existed at an early stage within each magma. The compositions of points *X* and *Y* are represented on the stereograms of figures 9 and 10. It will be seen that the point *X* falls outside the area enclosed by the dotted line on each stereogram, indicating that even though the vector communalities for these compositions are high (and so the projections were minor), the projected vectors represent compositions that are partly negative. The points labeled *Z* in figures 9 and 10 define vectors most like vectors *X* that are entirely nonnegative.

The compositions represented by points *Z* and *Y* (or *ABH* and *ANH*, respectively) in figures 9 and 10 are given in tables 11 and 12 for the Sierra Nevada and Alaska-Aleutian Range batholiths, respectively. It will be noted that the compositions given for vectors *ANH* in these tables differ from those given for points *Y* in figure 11. The differences are the result of projection of vectors representing the compositions given for points *Y* into the three-dimensional vector systems.

The compositions for vectors *ANH* are interpreted as those of assemblages that consist largely of calcic (anorthitic) plagioclase, hornblende, and possibly other mafic minerals. The compositions given for vectors *ABH* in tables 11 and 12 are interpreted as those of mineral assemblages that consist largely of intermediate (more albitic) plagioclase and hornblende. These compositions are reflected in the vector names.

Although the minimum acceptable communality (0.98) used in searching the hornblende-albite-anorthite-magnetite tetrahedron was selected somewhat arbitrarily, the selection does not have any important consequences on the final models or geologic interpretation. If the selected critical value is much less than 0.98, the silica contents of the *ANH* end members will be improbably low; if much greater than 0.98, the range of compositions for the mafic assemblages becomes improbably small.

Further development of the models for the two batholiths will rest on the assumption that the mineral assemblages that separated from the magmas that formed each batholith ranged in composition from

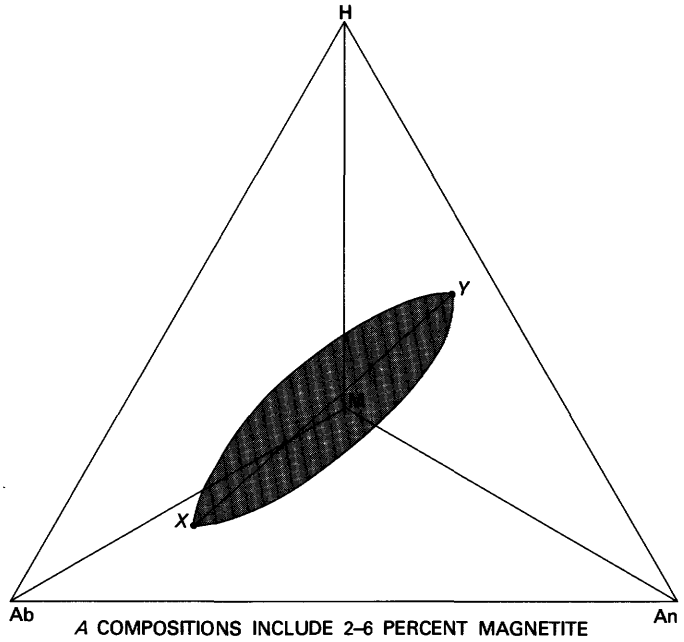

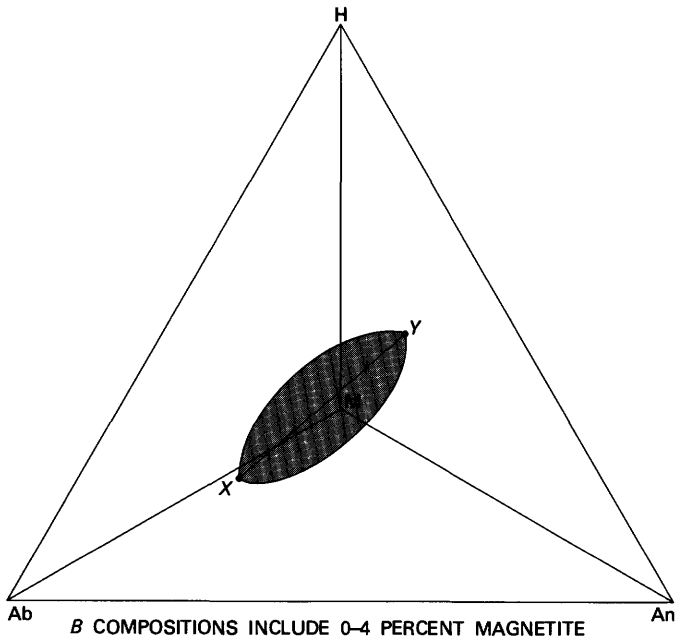

FIGURE 11.—Fields of composition (shaded) for the Sierra Nevada (*A*) and Alaska-Aleutian Range (*B*) batholiths in the hornblende-albite-anorthite-magnetite (H-Ab-An-M) system that have communalities higher than 0.98 when represented as vectors in the three-dimensional vector systems of figures 9 and 10, respectively. Fields have been projected from the magnetite (M) apex, in the foreground, onto the base of the tetrahedron. See table 10 for composition of the hornblende. The lines *X-Y* show the trends of compositions represented by vectors with the highest communalities.

TABLE 11.—*Chemical and normative compositions (weight percent) of end members for the three-end-member Sierra Nevada batholith model*

A. **Chemical compositions**

End member	SiO_2	Al_2O_3	'FeO'	MgO	CaO	Na_2O	K_2O
MGM	55.21	19.60	8.43	3.81	8.16	3.66	1.14
ABH	53.95	20.60	8.57	3.75	8.59	4.53	0
ANH	41.05	21.94	14.27	7.07	13.13	1.60	.93

B. **Normative compositions**[1]

End member	Q	Or	Ab	An	Lc	Ne	Wo	En	Fs	Fo	Fa	Cs
MGM ..	0.8	6.7	31.0	33.7	0	0	2.8	9.5	15.5	0	0	0
ABH ...	0	0	38.3	35.9	0	0	2.8	6.3	10.5	2.2	4.0	0
ANH ...	0	0	0	49.9	4.3	7.3	2.2	.9	1.3	11.7	19.2	3.1

[1]Normative mineral molecule abbreviations used throughout this report are as follows: Q, quartz; Or, orthoclase; Ab, albite; An, anorthite; Lc, leucite; Ne, nephelite; Wo, wollastonite; En, enstatite; Fs, ferrosilite; Fo, forsterite; Fa, fayalite; Cs, Ca_2SiO_4.

TABLE 12.—*Chemical and normative compositions (weight percent) of end members for the Alaska-Aleutian Range batholith model*

A. **Chemical compositions**

End member	SiO_2	Al_2O_3	'FeO'	MgO	CaO	Na_2O	K_2O
MGM	53.58	20.27	8.37	4.73	8.84	3.81	0.60
ABH	54.58	20.40	7.66	4.24	8.69	4.43	0
ANH	45.09	21.25	11.83	7.06	11.49	2.58	.70

B. **Normative compositions**

End member	Or	Ab	An	Ne	Wo	En	Fs	Fo	Fa
MGM	3.6	32.2	35.9	0	3.3	8.2	10.7	2.5	3.6
ABH	0	37.5	35.8	0	3.1	9.0	11.9	1.1	1.6
ANH	4.2	8.6	44.3	7.2	5.3	2.4	2.9	10.7	14.5

ABH to *ANH* as given in tables 11 and 12. The separated minerals, with total compositions in this range, will be referred to hereafter as mafic assemblages, or mafic-mineral assemblages, even though plagioclase of variable composition is interpreted to be a major component.

With this assumption, it is possible to define a range of compositions possible for the parent magmas or magma-source materials. It is necessary that the

Constituent	Compositions represented by points *X* and *Y*			
	Sierra Nevada		Alaska-Aleutian Range	
	X	*Y*	*X*	*Y*
SiO_2	59.87	46.36	57.26	48.06
Al_2O_3	21.14	19.55	20.92	19.89
'FeO'	3.97	12.21	5.28	11.22
MgO	1.51	6.27	2.51	5.52
CaO	5.50	13.79	7.29	12.65
Na_2O	7.93	1.48	6.60	2.36
K_2O	.08	.34	.14	.30

magma compositions be represented by vectors to the right-hand side of planes passing through vectors *ABH* and *ANH* in figures 9 and 10. Otherwise, the magma would have to be subtracted from the mafic assemblages in order to arrive at the compositions represented by the sample vectors. Moreover, it is necessary that vectors representing the magma compositions occur to the left of planes passing through points *ABH* and *MGM* and points *ANH* and *MGM*. Otherwise, (1) the composition of the mafic assemblages required to form some samples will not be in the range *ABH* to *ANH* (tables 11 and 12), or (2) the mafic assemblages would have to be added to the magma rather than separated from it. The vector represented by point *MGM* is the vector of intersection of a plane through vectors *ABH* and a vector representing a sample of extreme composition with another plane through vector *ANH* and another extreme sample vector (figs. 9 and 10). Thus, the only possible magma compositions are those that can be represented by vectors intermediate to vectors *MGM, ABH,* and *ANH* on figures 9 and 10. Accordingly, the only possible magma compositions are linear combinations of the compositions given for *MGM, ABH,* and *ANH* in tables 11 and 12. Vector *MGM* is chosen to represent the parent magma composition for each batholith because these compositions are most like the sample compositions and require the least magmatic differentiation to form each of the samples.

The compositions represented by the *MGM* vectors in figures 9 and 10, as given in tables 11 and 12, closely resemble the average composition of andesite tabulated by Nockolds (1954, p. 1019) except for the high values for Al_2O_3, the low value for MgO in the case of the Sierra Nevada batholith (table 11), and the low value for K_2O in the case of the Alaska-Aleutian Range batholith (table 12). Nockold's average andesite, with total iron as 'FeO' and recalculated to 100 percent, is SiO_2=55.85, Al_2O_3=17.69, 'FeO'=8.88, MgO=4.49, CaO=8.16, Na_2O=3.78, and K_2O=1.14. Thus, the starting materials for the generation of the batholiths will be taken as alumina-rich andesitic magmas or magma-source materials.

The compositions of the three end members for each batholith, as given in tables 11 and 12, can be used to approximate the compositions of all 228 samples from the Sierra Nevada and all 158 samples from the Alaska-Aleutian Range. The required mixing proportions are positive for end member *MGM*, representing the parent magma or magma-source material, and negative for end members *ABH* and *ANH*. There is only one exception; sample 72 from the Alaska-Aleutian Range (fig. 10) requires the separation of mafic assemblages that have compositions outside the range from *ABH* to *ANH*. That is, all but one of the sample compositions can be approximated by starting with $1+p$ parts magma, of composition *MGM*, and subtracting p parts of mafic assemblages that are intermediate in composition between end members *ABH* and *ANH*. The one exception, sample 72 (See Reed and Lanphere, 1974, table 1), is of a poorly exposed amphibolite and consists of 98 percent hornblende and calcic plagioclase. It might represent a metamorphosed gabbro of Jurassic age or, possibly, a material of the same origin as the smaller mafic inclusions present throughout many parts of the batholith.

Statistical summaries of the mixing proportions required for the individual samples are given in tables 13 and 14. Just as the individual sample compositions can be approximated by combining the end-member compositions in proportions determined for each sample, the average compositions for each group of plutons, as given in tables 6 and 7, can be approximated by combining the end-member compositions in the average proportions given for each group in tables 13 and 14. If either of these approximations are derived, it will be seen that they are only moderately good for Al_2O_3, Na_2O, and K_2O in the Sierran rocks. This is in accord with the factor-variance diagram in figure 7, which indicates that three-end-member models for the Sierra Nevada batholith account for these oxides to a lesser degree than they account for others. Hence, a four-end-member model will be sought.

As shown by the factor-variance diagrams in figures 7 and 8, a fourth end member is required for the Sierra Nevada model in order to account for the compositional variability to about the same degree that a three-end-member model accounts for the variability in the Alaska-Aleutian Range batholith. The reason for this is not clear, and the selection of a fourth end member for the Sierran model is difficult. However, studies of the chemical and isotopic variations in the granitic rocks led Kistler and Peterman (1973) to suggest that the parent magmas were derived from deep-seated materials that varied laterally in composition. If their interpretation is correct, the fourth end member might appropriately allow for compositional variations among the parent magmas or within the magma-source material. The average composition of all the magmas, or of the magma-source material, is taken as that of *MGM* in table 11. It remains only to find the manner in which the compositions varied. The major variation is expected to have been in a direction generally perpendicular to the continental margin.

An extreme parent-magma composition was sought by using the average composition of samples from the

TABLE 13.—*Statistical summary of mixing proportions for the three-end-member Sierra Nevada Batholith model*

[See table 11 for compositions of end members *MGM, ABH* and *ANH*]

Group of plutons	Number of samples	Averages			Standard deviations		
		MGM	*ABH*	*ANH*	*MGM*	*ABH*	*ANH*
White Mountains rocks	21	3.95	-2.19	-0.76	0.54	0.39	0.22
Palisade Crest sequence	19	3.79	-2.09	-.69	.65	.53	.19
Scheelite sequence	23	4.81	-2.86	-.94	.69	.48	.26
Toulumne intrusive series	7	3.73	-1.84	-.89	1.15	.99	.17
Yosemite rocks	7	4.39	-2.31	-1.07	.93	.81	.15
Shaver sequence	36	4.17	-2.32	-.85	.91	.65	.31
All other plutons	115	3.76	-1.97	-.80	.89	.64	.28
All plutons	228	3.97	-2.16	-.82	.89	.67	.27

TABLE 14.—*Statistical summary of mixing proportions for the Alaska-Aleutian Range Batholith model*

[See table 12 for compositions of end members *MGM, ABH* and *ANH*]

Group of plutons	Number of samples	Averages			Standard deviations		
		MGM	*ABH*	*ANH*	*MGM*	*ABH*	*ANH*
Merrill Pass sequence	29	10.48	-6.23	-3.25	1.47	1.07	0.41
Quartz monzonite of Tired Pup	14	11.22	-7.04	-3.17	.92	.68	.27
Crystal Creek sequence	22	10.44	-6.25	-3.18	.95	.67	.30
Hartman sequence	5	8.30	-5.21	-2.09	.93	.85	.09
Granodiorite of Mount Estelle	13	8.47	-5.26	-2.20	.84	.56	.31
Yentna sequence	8	8.02	-5.06	-1.96	1.61	1.12	.53
Summit Lake rocks	35	4.65	-2.09	-1.57	1.64	1.15	.60
Undivided plutonic rocks	3	9.31	-5.74	-2.57	1.43	.74	.73
Plutonic rocks of Jurassic age.	[1]28	4.46	-2.13	-1.33	1.85	1.27	.79
All plutons	[1]157	7.73	-4.44	-2.29	3.15	2.25	.98

[1]Sample 72 was excluded. See text.

White Mountains, (the easternmost group of plutons in the Sierra Nevada), as given in table 6, in order to estimate the magma composition required for this easternmost group of plutons. This average composition from table 6 is used to form a row vector, *W*. According to the three-end-member Sierran model, composition *W* resulted largely from the separation of mafic assemblages from a parent magma, or magma-source material. The average composition of the mafic assemblages was equal to a mixture of 2.19 parts *ABH* and 0.76 parts *ANH* (tables 11 and 13), and 3.95 parts of initial magma were required (1.00+2.19+0.76). The following approximate matrix equation can be written:

$$3.95U - AF \approx W, \text{ or}$$
$$U \approx (W + AF)/3.95.$$

The row vector *U* is the required magma composition for the White Mountains rocks, *A* is a row vector containing the mixing proportions for *ABH* and *ANH* (2.19 and 0.76) from table 13, and *F* is a matrix (with 2 rows and 7 columns) containing the compositions of end members *ABH* and *ANH* from table 11. Solution of the approximation for *U* gives:

Weight percent						
SiO_2	Al_2O_3	'FeO'	MgO	CaO	Na_2O	K_2O
54.73	19.79	8.47	3.83	8.11	3.73	1.33

This composition was represented as a vector in the seven-dimensional vector space for the Sierra Nevada samples and projected into the four-dimensional vector system. The communality of the vector after projection was 0.99999, indicating that the composition, *U*, is highly compatible with the compositional variability among the Sierran samples. The composition of the vector representing composition *U*, after projection of the vector into the four-dimensional vector system, differs from composition *U* only in the second decimal places.

The composition of end member *MGM* (table 11) was also represented as a vector in the four-dimensional vector system, and the assumption was made that the two vectors to represent the extreme compositions among the parent magmas, or magma-source materials, occur in the plane of the *U* and *MGM* vec-

tors. The two vectors representing the extreme magma compositions, *MGM*1 and *MGM*2, were taken as two extreme vectors in this plane. Each extreme vector was such that the mixing proportions for at least one sample indicated zero parts of the respective end member, and the mixing proportions for all other samples were positive for both of these end members. The compositions represented by these extreme vectors, *MGM*1 and *MGM*2 are given in table 15 along with the compositions of end members *ABH* and *ANH* from table 11. It will be seen that the compositional variation required among the magmas, or magma-source materials, is small; SiO_2 ranges only from 53.51 to 56.12 percent. The greatest proportional variation, by far, is for K_2O (0.77 to 1.81 percent), which is in accord with compositional variations among the granitic rocks as described by Bateman and Dodge (1970).

TABLE 15.—*Chemical and normative compositions (weight percent) of end members for the four-end-member Sierra Nevada batholith model*

A. Chemical compositions

End member	SiO_2	Al_2O_3	'FeO'	MgO	CaO	Na_2O	K_2O
*MGM*1 ...	53.51	20.26	8.64	3.86	8.01	3.90	1.81
*MGM*2 ...	56.12	19.24	8.31	3.78	8.24	3.53	.77
ABH	53.95	20.60	8.57	3.75	8.59	4.53	0
ANH	41.05	21.94	14.27	7.07	13.13	1.60	.93

B. Normative compositions

End member	Q	Or	Ab	An	Lc	Ne	Wo	En	Fs	Fo	Fa	Cs
*MGM*1 .	0	10.7	33.0	32.4	0	0	3.1	2.7	4.4	4.9	8.8	0
*MGM*2 .	3.8	4.6	29.9	34.4	0	0	2.7	9.4	15.3	0	0	0
ABH ...	0	0	38.3	35.9	0	0	2.8	6.3	10.5	2.2	4.0	0
ANH ...	0	0	0	49.9	4.3	7.3	2.2	.9	1.3	11.7	19.2	3.1

The compositions of each of the 228 samples from the Sierra Nevada can be closely approximated (to the degree indicated for a four-end-member model by figure 7) by mixing end members *MGM*1 and *MGM*2 in positive proportions and subtracting mixtures of *ABH* and *ANH* (table 15). A statistical summary of the mixing proportions is given in table 16. In addition, the average compositions for groups of plutons, given in table 6, can be approximated with this model (as was done with the three-end-member model in table 13) by combining the end-member compositions in table 15 according to the average proportions given in table 16.

In summary, the major part (more than 92 percent) of the compositional variability in the Alaska-Aleutian Range batholith can be accounted for by starting with an andesitic magma, or magma-source material, with the composition of *MGM* in table 12, and subtracting varying amounts of mafic mineral assemblages that range in composition from that of *ABH* and *ANH*, also given in table 12. A basically similar model will account for the major part (more than 90 percent) of the compositional variability in the Sierra Nevada batholith, but it is necessary to allow some variation in the composition of the andesitic parent magma or magma-source material. Table 17 was derived from the mixing proportions for end members *MGM*1 and *MGM*2 (table 16) and the compositions of these end members (table 15) and shows the average composition of the parent magmas required by the model for the samples from each group of plutons. The greatest proportional variation among these compositions is with respect to K_2O. The average composition required for the batholith as a whole (listed as "all plutons" in table 17) is precisely that proposed in the thee-end-member model (table 11).

The variation in K_2O among the magmas specified by the model for the various groups of plutons is small (table 17) but corresponds in a general way with the distance of the plutons from the continental margin. (See map of Bateman and Dodge, 1970, fig. 2.) This is in accord with the proposal of Moore (1959) that the source materials for granitic rocks of the western U.S. had K_2O contents that increased progressively away from the continental margin.

The average compositions of the mafic assemblages separated from the magma, or magma-source material, for each batholith are given in table 18. These average compositions were computed from the average mixing proportions for end members *ABH* and *ANH* (tables 14 and 16) and the compositions of these end members (tables 12 and 15). If the mafic assemblages are represented by the mafic inclusions that are widespread throughout many parts of both batholiths, the average compositions of the assemblages and the inclusions should be similar. Unfortunately, few data are available on the compositions of the inclusions in either batholith. However, Morton, Baird, and Baird (1969, p. 1558) gave the average composition of 13 similar inclusions from a pluton in the southern California batholith. This average composition (recomputed to percents of oxides) is given in table 18 and is generally similar to the average compositions of the mafic assemblages derived from the factor models for both batholiths.

The average mixing proportions for the *MGM* end member as given in table 14 indicate that, according to the model, the Alaska-Aleutian Range batholith form-

TABLE 16.—*Statistical summary of mixing proportions for the four-end-member Sierra Nevada batholith model*

[See table 15 for composition of end members *MGM1*, *MGM2*, *ABH*, and *ANH*]

Group of plutons	Number of samples	Averages				Standard deviations			
		MGM1	*MGM2*	*ABH*	*ANH*	*MGM1*	*MGM2*	*ABH*	*ANH*
White Mountains rocks	21	2.12	1.83	-2.18	-0.76	0.50	0.66	0.43	0.23
Palisade Crest sequence	19	1.65	2.14	-2.10	-.69	.48	.53	.57	.20
Scheelite sequence	23	1.56	3.23	-2.85	-.94	.53	.72	.46	.25
Toulumne intrusive series	7	1.35	2.38	-1.84	-.89	.44	.77	.99	.17
Yosemite rocks	7	1.19	3.19	-2.32	-1.06	.50	.52	.78	.15
Shaver sequence	36	1.26	2.92	-2.32	-.85	.47	.54	.64	.30
All other plutons	115	1.25	2.52	-1.97	-.80	.45	.56	.63	.27
All plutons	228	1.40	2.57	-2.15	-.82	.53	.69	.66	.27

TABLE 17.—*Average compositions, in percent, of magmas for the Sierra Nevada batholith model*

Group of plutons	SiO_2	Al_2O_3	'FeO'	MgO	CaO	Na_2O	K_2O
White Mountains rocks	54.72	19.79	8.49	3.82	8.12	3.73	1.33
Paliade crest sequence	54.99	19.69	8.45	3.82	8.14	3.69	1.22
Scheelite sequence	55.28	19.57	8.42	3.81	8.17	3.65	1.11
Toulumne intrusive series	55.18	19.61	8.43	3.81	8.16	3.66	1.15
Yosemite rocks	55.42	19.52	8.40	3.80	8.18	3.63	1.05
Shaver sequence	55.34	19.55	8.41	3.80	8.17	3.64	1.08
All other plutons	55.26	19.58	8.42	3.81	8.16	3.65	1.11
All plutons	55.21	19.60	8.43	3.81	8.16	3.66	1.14

TABLE 18.—*Compositions of mafic-mineral assemblages (end members* ABH *and* ANH *required for the average samples from the two batholiths according to the derived models, and the average composition of mafic inclusions from the southern California batholith*

Constituent	Average composition (in percent)		
	Mafic mineral assemblages		Mafic inclusions[1]
	Alaska-Aleutian Range batholith	Sierra Nevada batholith	
SiO_2	51.35	50.39	51.67
Al_2O_3	20.69	20.97	19.31
'FeO'	9.08	10.14	8.62
MgO	5.20	4.67	5.34
CaO	9.64	9.84	9.19
Na_2O	3.80	3.72	3.01
K_2O	.24	.26	1.30

[1]Average of 13 analyses of samples from the Lakeview Mountains pluton (Morton and others, 1969, table 4).

ed from a starting material (magma or magma-source material) with a mass of about 7.73 times the mass of the part of the batholith represented by the 158 samples. Thus, the batholith represents about 12.94 (100/7.73) percent of the starting material. (Here and throughout the remainder of this report, many of the reported computational results contain more significant figures than are justified by the data. The additional figures are retained in order to allow the reader to follow the nature of the computations more easily.) A similar calculation for the Sierra Nevada batholith, based on the mixing proportions for all plutons given in tables 13 and 16, indicates that the batholith formed from about 25.19 percent of the starting material.

FORMATION OF AN INDIVIDUAL PLUTON

The models presented for the Sierra Nevada and Alaska-Aleutian Range batholiths call for a magma or source material of andesitic composition, and for subsequent separation of mafic mineral assemblages. However, field studies have revealed very clearly that mafic minerals not only separated from the magma, but accumulated in the marginal parts of many plutons, at least partly by accretion on the walls of the magma conduit (Bateman and others, 1963, p. D30–D31; Presnall and Bateman, 1973, p. 3196-3197). In fact, some samples from the marginal parts consist of collections of plagioclase, hornblende, and biotite with little quartz and essentially no potassium feldspar, even through potassium feldspar is abundant in the pluton's central part. The question here is how this process of crystal accumulation can be reconciled with a model that calls for a net loss of mafic mineral assemblages. (See mixing proportions in tables 13, 14, and 16.)

A possible explanation is given in figure 12. Figures 12*A* and 12*B* are stereograms of the same type given in figures 2, 9, and 10. Figure 12*A* shows a representation of the earliest stages of the process. Vector *MGM* represents the composition of the parent magma, or magma-source material. Separation of mineral assemblages ranging in composition from *a* to *b* could change the magma composition to range from *c* to *d*. Composition *c* would result from the separation of

2.746 parts of composition *b* from 3.746 parts of composition *MGM*. Composition *d* would result from the separation of 3.360 parts of composition *a* from 4.360 parts of composition *MGM*. The modified magma, therefore, would represent about one-fourth of the original magma or magma-source material. The compositional variation in the mixture is small (ranging from *c* to *d* in fig. 12), but could have resulted from minor compositional variations in the separated mafic assemblages as represented in figure 12*A*. This variation, in turn, might have been caused by temperature and density gradients within the ascending magma.

The solid points in figure 12*B* represent vectors that correspond to the compositions of samples from the Mt. Givens pluton in the central part of the Sierra Nevada (Bateman and others, 1963). Some of these samples are more felsic than the melt (points to the right of plane *c-d*), and some are more mafic (points to the left of plane *c-d*). Those that are more felsic may have formed by the separation of mafic minerals from the magma, and those more mafic formed by addition of the mafic minerals. For example, sample *e* might have formed by the subtraction of 0.115 parts of composition *h* from 1.115 parts of composition *d*. Sample *f* might have formed from the addition of 0.118 parts of composition *g* to 0.882 parts of composition *c*. Other samples, farther to the left of plane *c-d* and closer to the plane *ABH-ANH*, could result from the accumulation of mafic minerals containing only the amounts of melt that would occupy the mineral interstices.

The composition loadings, or mixing proportions, summarized in tables 13, 14, and 16 may reflect the net

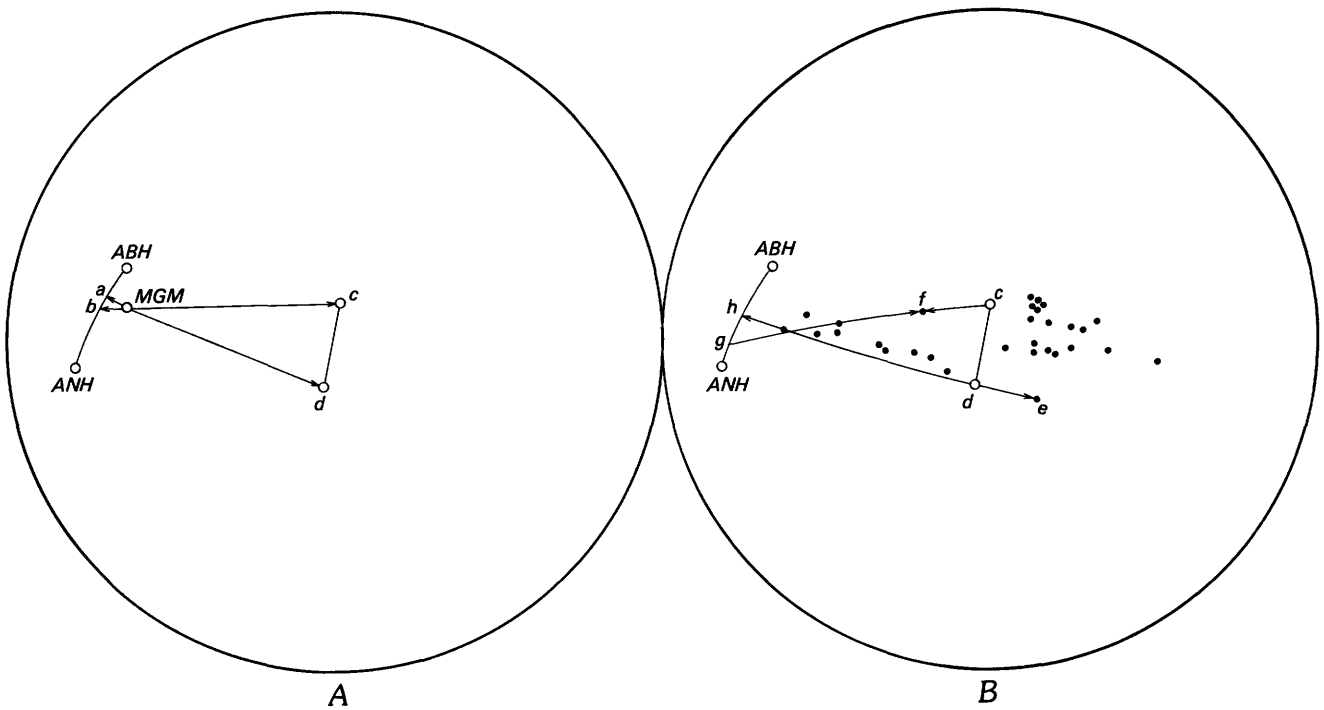

FIGURE 12.—Vector diagrams representing a process of formation of the magma for the Mount Givens pluton of the Sierra Nevada batholith (*A*), and a process of differentiation of the magma (*B*). The magma may have ranged in composition from *c* to *d*, resulting from the separation of mafic assemblages from the magma, *MGM*. The mafic assemblages ranged in composition from *a* to *b*. At a later stage, *B*, the magma differentiated by separation of mafic minerals (composition *h*) from some part of the magma (composition *d*) to form sample *e*, and by addition of mafic minerals (composition *g*) to another part (composition *c*) to form sample *f*.

Constituent	Compositions represented by vectors, in percent										
	ABH	*ANH*	*MGM*	*a*	*b*	*c*	*d*	*e*	*f*	*g*	*h*
SiO_2	53.95	41.05	55.21	50.96	49.86	69.88	69.49	71.69	67.17	46.97	50.28
Al_2O_3	20.60	21.94	19.60	20.91	21.03	15.69	15.18	14.52	16.35	21.33	20.98
'FeO'	8.57	14.27	8.43	9.89	10.38	3.06	3.49	2.72	4.08	11.66	10.20
MgO	3.75	7.07	3.81	4.52	4.81	1.06	1.40	1.02	1.59	5.55	4.70
CaO	8.59	13.13	8.16	9.64	10.03	3.03	3.18	2.41	3.98	11.05	9.88
Na_2O	4.53	1.60	3.66	3.85	3.60	3.83	3.03	2.95	3.73	2.95	3.70
K_2O	0	.93	1.14	.22	.30	3.44	4.24	4.69	3.10	.51	.27

effects of a two-stage process such as that represented in figure 12. This explanation requires that all separated mineral assemblages, both those separated early and those separated later, have total compositions in the range from *ABH* to *ANH*. However, if this were not the situation, the compositional structures in the batholiths would be more complex than indicated by the factor-variance diagrams in figures 7 and 8.

COMPOSITIONS OF PARTIAL MELTS FROM THE CRUST

Presnall and Bateman (1973) gave evidence that a major portion of the Sierra Nevada batholith originated by equilibrium fusion of the lower crust. The fusion processes caused the development of a crystal-liquid mush, the crystal portion consisting mostly of the more refractory minerals. They proposed that as the degree of crustal fusion reached some point, the crystal-liquid mush began to rise, and at least some of the crystal portion of the mush was retained in the liquid all the way to the observed sites of magma emplacement. Other parts of the crystalline material were either left behind at the sites of fusion or settled out of the mush, perhaps to form the mafic inclusions widespread throughout much of the batholith (Presnall and Bateman, 1973, p. 3197).

If the model of Presnall and Bateman and the factor model for the Sierra Nevada are both correct, certain consequences follow from the factor model regarding the compositions of the melts formed in the crust, the degree of melting, and the proportions of refractory material retained in the melt or precipitated from it. These consequences are described here so that they may be used in evaluating the models for both batholiths at some future time when more is known about the physicochemical aspects of the melting process and the conditions of melting that may have produced these batholiths. Experimental studies of melting have been directed at the petrologic system quartz-K-feldspar-albite-H_2O, and at the artificial melting of mafic and ultramafic rocks. See James and Hamilton (1969) and Presnall and Bateman (1973, p. 3187-3190) for reviews of this work and extensive bibliographies.

Previously in this report, we have referred to the *MGM* (also *MGM*1 and *MGM*2) end members as representing either magma or magma-source material. If they represent magmas, the magmas must have been modified to the compositions of the samples by precipitation of mafic mineral assemblages within the compositional ranges from *ABH* to *ANH*. Alternatively, the models can be reconciled with the model of Presnall and Bateman by regarding the *MGM* end members as magma-source materials, rather than as magmas, and the *ABH* and *ANH* end members as representing the extremes in the range of refractory mineral assemblages. Thus, end members *MGM*1 and *MGM*2 (table 15) represent the range of compositions in the original crust beneath the Sierras, and the average compositions in table 17 indicate the average composition of the crustal materials that led to the formation of each group of plutons. Similarly, end member *MGM* for the Alaska-Aleutian Range model (table 12) represents a more uniform crustal material that originally may have been present beneath that batholith.

The factor models for the two batholiths specify the compositions of both the initial crustal materials and the mafic assemblages that comprise the more refractory phases. We do not know the abundance of the refractory phases in the partially melted crust or, from mathematical evidence alone, whether they were even present. If the melting of the crust had been nearly complete, for example, the refractory phases would have nearly disappeared. In this situation, the composition of the melt would have been close to the composition of the *MGM* end member and would have had to have been modified to the observed compositions of the samples by precipitation of mafic mineral assemblages. If, on the other hand, the degree of melting had been low, the composition of the melt would have been highly salic, and some refractory material (mafic assemblages) would have had to have been retained in the melt in order to produce the observed samples. Thus, it is only possible to estimate a range of melt compositions that could have led to each sample. The method of estimation will be illustrated for the theoretical average sample from the Alaska-Aleutian Range batholith.

The derived average composition of the crust originally beneath the Alaska-Aleutian Range is given in column (*a*) of table 19, and the average composition of the separated mafic assemblages is given in column (*b*). If we assume minimum melting, and therefore minimum heat requirements, we will wish to retain as much of the crust as possible in the form of crystalline mafic assemblages. However, the proportion of crystalline material is limited by the relative MgO contents of the crust and the assemblages (columns *a* and *b*); if more than 90.96 percent of the crust consisted of the crystalline assemblages, the derived MgO content of the liquid portion would be negative. Columns (*c*) and (*d*) give the composition of the crystal-liquid mush—with the assumption of minimum melting—separated according to crystal and liquid portions. Column (*c*) was computed as 90.96 percent of column (*b*) and column (*d*) was derived as the difference between columns (*a*) and (*c*). Therefore, if the model is

interpreted in terms of partial melting of the crust, it must be concluded that at least 9.04 percent (table 19*A*, column *d*) of the crust had to melt to produce refractory-mineral assemblages of the composition given in column (*b*). The composition of the liquid portion of the mush is given in column (*e*), which simply shows the data from column (*d*) recalculated to 100 percent.

The average mixing proportions given in table 14 indicate that the Alaska-Aleutian Range batholith as a whole formed from 7.73 parts crust (in the context of this discussion), from which 6.73 parts of mafic assemblages separated. Thus, the batholith formed from 12.94 (100/7.73) percent of the crust. The computations that led to column (*d*) of table 19*A*, however, show that the melt, under minimum melting conditions, formed from only 9.04 percent of the crust. The difference, 3.90 percent, must have consisted of refractory-mineral assemblages that were retained and carried upward in the rising liquid. The refractory material, then, would have comprised 30 percent (100×3.90/12.94) of the liquid-crystal mixture. The total composition of the liquid plus retained crystals is derived in columns (*f*) and (*g*) and closely approximates the average composition of the total batholith given in column (*h*). Columns (*f*), (*g*), and (*h*) merely serve as a check on the computations. The values in column (*e*) are of the most interest; they show the composition of the melt under conditions of minimum melting as derived from the Alaska-Aleutian Range model. The normative composition of the melt is 96 percent $Q_{36}Or_{26}Ab_{34}An_4$.

The computations shown in table 19*A* are based on the assumption that the degree of melting in the crust was minimal (9.04 percent) so that the melt contained no MgO. Similar computations can be made with assumptions that the degree of melting was greater. An example, based on the assumption of 20 percent crustal melting is given in table 19*B*. The derived melt composition (column *e*) is less siliceous than that derived in table 19*A*, and it is necessary to precipitate 7.06 percent mafic assemblages in order to form the batholith from 12.94 percent of the crust (20−12.94=7.06). See table 19*B*, column (*f*). This constitutes precipitation of 35.3 percent of the melt fraction (100×7.06/20=35.3).

Computations similar to those outlined in table 19 were carried out for each of the 158 individual samples from the Alaska-Aleutian Range batholith and for the average composition of each group of plutons listed in table 7. The composition of the crust used for each computation was the same as that given in column (*a*)

TABLE 19.—*Mass balance computations for the average sample from the Alaska-Aleutian Range batholith*

Constituent	(*a*) Composition of crust (*MGM* from table 12)	(*b*) Average composition of mafic assemblages[1]	(*c*) Crystal-liquid mixture: Crystals	(*d*) Crystal-liquid mixture: Liquid (column *a* minus column *c*	(*e*) Composition of partial melt (column *d* recalculated to 100	(*f*) Liquid plus (or minus) crystals	(*g*) Column *f* recalculated to 100	(*h*) Average composition of batholith (from table 5)
A. Assuming the lowest possible degree (9.04 percent) of crustal melting;			Column *c* = 0.9096 × column *b*			Column *f* = column *d* +0.0390 × column *b*		
SiO_2	53.58	51.35	46.71	6.87	76.0	8.87	68.5	68.60
Al_2O_3	20.07	20.69	18.82	1.25	13.8	2.06	15.9	15.89
'FeO'	8.37	9.08	8.26	.11	1.2	.46	3.6	3.62
MgO	4.73	5.20	4.73	0	0	.20	1.5	1.53
CaO	8.84	9.64	8.77	.07	.8	.45	3.5	3.44
Na_2O	3.81	3.80	3.45	.36	4.0	.51	3.9	3.87
K_2O	.60	.24	.22	.38	4.2	.39	3.0	3.05
Total	100.00	100.00	90.96	9.04	100.00	12.94	99.9	100.00
B. Assuming 20 percent crustal melting;			Column *c* = 0.80 × column *b*			Column *f* = column *d* −0.0706 × column *b*		
SiO_2	53.58	51.35	41.08	12.50	62.5	8.87	68.5	68.60
Al_2O_3	20.07	20.69	16.55	3.52	17.6	2.06	15.9	15.89
'FeO'	8.37	9.08	7.27	1.10	5.5	.46	3.6	3.62
MgO	4.73	5.20	4.16	.57	2.9	.20	1.5	1.53
CaO	8.84	9.64	7.71	1.13	5.6	.45	3.5	3.44
Na_2O	3.81	3.80	3.04	.77	3.9	.51	3.9	3.87
K_2O	.60	.24	.19	.41	2.0	.39	3.0	3.05
Total	100.00	100.00	80.00	20.00	100.00	12.94	99.9	100.00

[1]Equals a mixture of 4.44 parts of end member *ABH* and 2.29 parts of end member *ANH* (tables 12 and 14), recalculated to 100 percent.

of table 19 and the compositions of the mafic assemblages (column *b*) were derived from the mixing proportions for end members *ABH* and *ANH* as computed for the individual samples and for the average sample from each group of plutons (table 14). The CIPW norms were computed for each derived melt composition, and the normative values for Q, Or, Ab, and An were adjusted to sum to 100 percent. These adjusted values were then represented in a Q-Or-Ab-An tetrahedron and were found to define a surface as shown in figure 13. (Only 5 of the 158 samples gave results that deviated from this surface.) The surface contains all possible melt compositions that can be derived from the model assuming degrees of crustal melting ranging from the minimum for each sample to 100 percent. The possible melt compositions for each individual sample occur on a line within the surface that extends from the line *x-y-z* to the point *MGM*. These lines are shown in figure 13 for the average of all samples from the batholith (line *a-MGM*) and for the average sample from each group of plutons. The two extreme samples are represented by lines *x-MGM* and *z-MGM*. The extreme sample represented by line *z-MGM* could have formed with as little as 5.6 percent

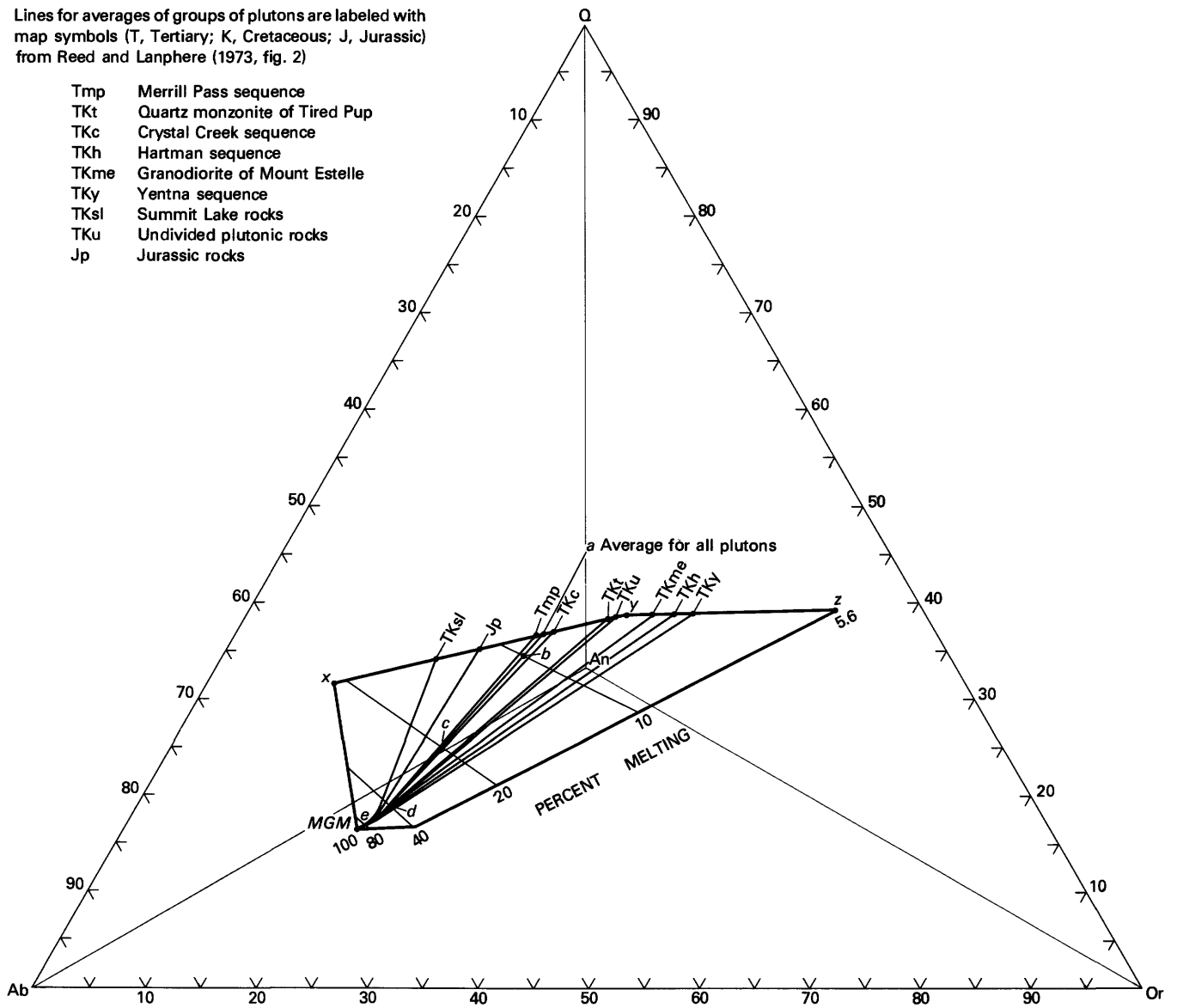

FIGURE 13.—Q-Or-Ab-An tetrahedron showing the surface containing possible melt compositions for samples from the Alaska-Aleutian Range batholith. The possible melt compositions were determined from the model by assuming various degrees of melting in the crust. The tetrahedron is viewed from directly above with the An apex in the foreground. The lines connecting the point *MGM* with the points for individual groups of plutons define the ranges of possible melt compositions for the average sample from each group. See table 20 for positions of points within the tetrahedron and other data.

melting in the crust, whereas the sample represented by line *x-MGM* requires crustal melting of at least 23.7 percent. The surface shown in figure 13 is essentially planar in the range from 5.6 percent to more than 40 percent melting and is curved convexly upward near the Ab-An-Or face of the tetrahedron. Data pertaining to each of the labeled points in figure 13 are given in table 20. The data for the average of all samples (line *a-MGM*) indicate that under minimum melting conditions the crustal melt retained 3.9 percent mafic assemblages and that if the degree of melting exceeded 10 to 20 percent (about 13 percent by interpolation), the mafic assemblages would have had to have been precipitated from the melt in order to modify the melt composition to that of the average composition of the batholith.

The lines in figure 13 containing the possible melt compositions for the average sample from each group of plutons (*TKsl-MGM, Jp-MGM*, and so forth) have positions that correspond in a general way to the geographic positions of the respective groups. The groups of plutons on the eastern margin of the batholith, nearer to the continental margin (Reed and Lanphere, 1973, fig. 2), tend to be represented by lines closer to the line *x-MGM* in figure 13. This indicates that, according to the model, groups of plutons that formed at a distance from the continental margin could have resulted from lower degrees of crustal melting than did those nearer the margin. The minimum degrees of melting for the average sample from each group are given in table 20; they range from 6.7 to 13.2 percent.

Computations similar to those outlined in table 19 and those used to construct figure 13 were also carried out for each individual sample from the 6 groups of Sierra Nevada plutons listed in table 6. The composi-

TABLE 20.—*Data pertaining to points within tetrahedron of figure 13*

Group of plutons	Point in fig. 13	Percent Q+Or+Ab+An in melt	Position of point in tetrahedron				Percent melting	Percent mafic assemblages retained in (+) or precipitated from (−) melt
			Q	Or	Ab	An		
All plutons	*z*	88.7	39	53	8	0	5.6	+19.4
Do	*y*	95.9	39	33	28	0	7.4	+0.8
Do	*x*	96.9	26	6	52	16	23.7	+3.3
Do	*a*	96.3	36	26	34	4	9.0	+3.9
Do	*b*	94.1	32	24	35	9	10.0	+2.9
Do	*c*	81.4	15	15	40	30	20.0	−7.1
Do	*d*	74.0	4	9	44	43	40.0	−27.1
Do	*e*	71.5	0	6	45	49	80.0	−67.1
Do	*MGM*	71.7	0	5	45	50	100.0	−87.1
Yentna sequence ..	TKy	93.4	39	40	21	0	6.7	+5.8
Hartman sequence	TKh	94.1	39	38	23	0	6.9	+5.2
Granodiorite of Mount Estelle.	TKme	94.9	39	36	25	0	7.1	+4.7
Undivided plutonic rocks.	TKu	96.1	39	33	28	0	7.5	+3.3
Quartz monzonite of Tired Pup.	Tkt	96.1	39	33	29	0	7.5	+1.4
Crystal Creek sequence.	TKc	96.3	36	27	34	4	8.9	+0.7
Merrill Pass sequence.	Tmp	96.3	36	26	35	4	9.2	+0.4
Jurassic rocks	Jp	96.5	33	20	40	8	11.2	+11.2
Summit Lake rocks	TKsl	96.6	31	16	43	10	13.2	+8.3

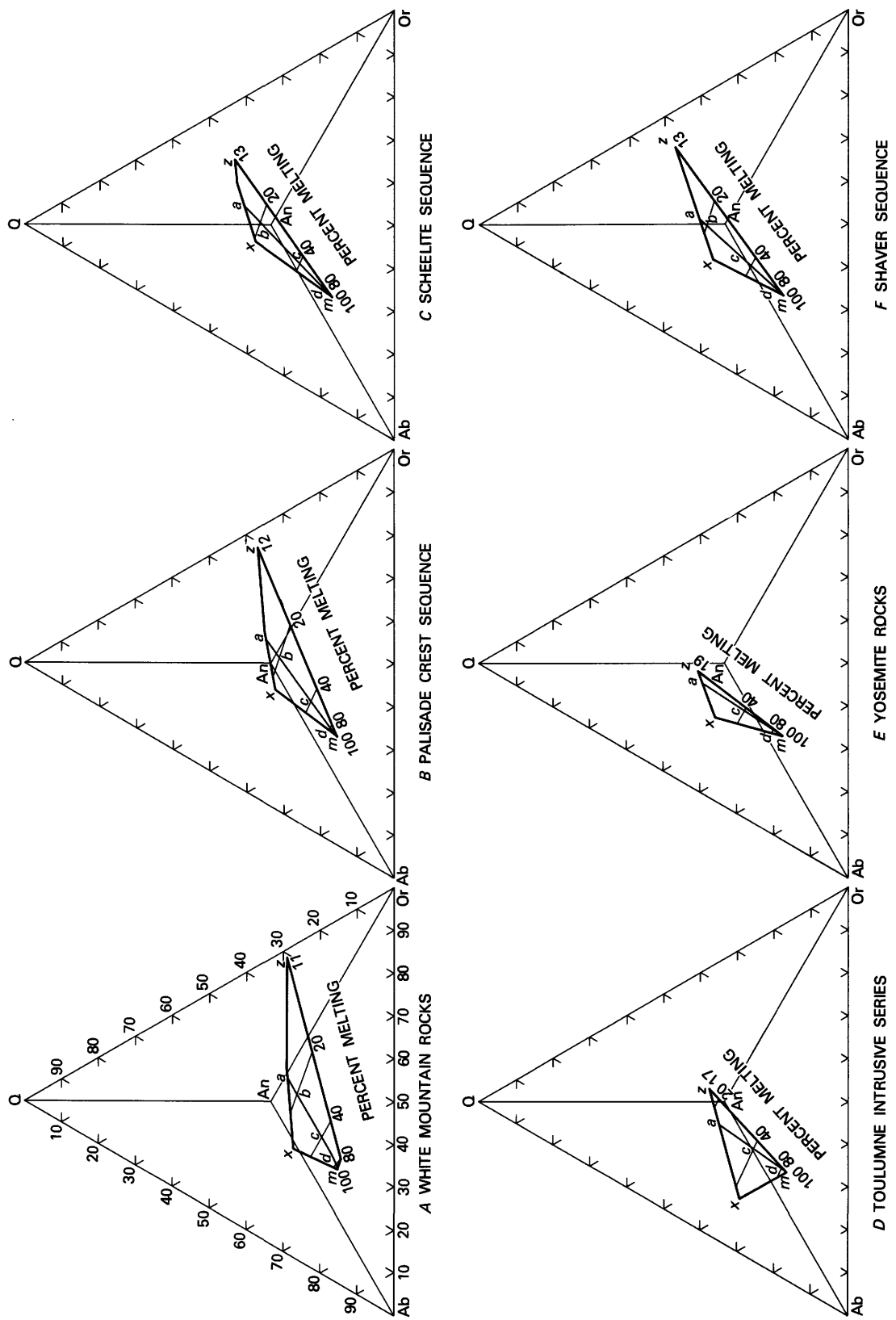

FIGURE 14.—Q-Or-Ab-An tetrahedrons showing the surfaces containing possible melt compositions for six groups of plutons within the Sierra Nevada batholith. The possible melt compositions were determined from the four-end-member model by assuming various degrees of melting in the crust. The tetrahedrons are viewed from directly above with the An apex in the foreground. The line *a-m* within each tetrahedron defines the range of possible melt compositions for the average sample from the corresponding group of plutons. See table 21 for positions of points within each tetrahedron and other data.

tions assumed for the crust, corresponding to column (*a*) in table 19, were different for each group of plutons and are given in table 17. The compositions of the mafic assemblages, corresponding to column (*b*) in table 19, were estimated from the mixing proportions for end members *ABH* and *ANH* for each sample and for the average sample from each group of plutons (table 16). The derived partial melt compositions occur within 6 different surfaces within the Q-Or-Ab-An tetrahedron, as shown in figure 14. Each of the surfaces is planar between the line representing minimum melting (*x-a-z*) and that representing melting of 80 percent. The possible melt compositions for the average sample from each group of plutons occur in the line *a-m* on each diagram. Each of these lines is close to the approximate trend of compositions of granites of the Sierra Nevada batholith shown by Presnall and Bateman (1973, line *m-n* in figure 4 of that report). The computations for individual samples indicate that the degree of melting ranged from 11 to 46 percent (11 to 27 percent for all but one sample) and that, in general, melting of more than about 25 percent necessitates the precipitation of mafic mineral assemblages (table 21).

The minimum degree of melting for the average sample from each group of Sierra Nevada plutons is given in table 21 (see point *a* for each group); these minimum values vary only from 16.5 to 21.2 percent. The positions of the lines *x-a-z* for the different groups within the Q-Or-Ab-An tetrahedron (fig. 14), however, vary in a way that might be significant. Each of the lines is approximately parallel to the cotectic lines separating the quartz and feldspar fields on experimentally derived phase diagrams. The cotectic lines for higher partial pressures of H_2O are farther from the quartz corner of the tetrahedron than are those for lower pressures. (See Luth and others, 1964, fig. 4; and Carmichael and others, 1974, p. 230.) If the melting process was one of equilibrium fusion, as concluded by Presnall and Bateman (1973), the initial melts may be expected to have had compositions near the cotectic lines. This would imply that the White Mountains rocks and the Palisade Crest sequence (figs. 14*A* and 14*B*) formed at higher pressures than did some of the other groups of plutons located closer to the continental margin where the crust is probably thinner.

It was stated previously that the factor models derived for the two batholiths are not unique, and it should be emphasized here that the observations described regarding the processes of melting and the resultant melt compositions are only as valid as the models themselves. These observations by no means confirm the validity of the models, but, on the other hand, do appear compatible with data from both field and experimental studies.

CONCLUSIONS

Igneous rock bodies that have formed by complex processes, involving the mixing and unmixing of a large number of end members, have complex compositional structures. Those that form, for example, by the mixing of a magma with only a few types of country rock or by the separation of only a few mineral phases from a magma, have simple compositional structures. The type of compositional structure in a rock body is revealed by a factor-variance diagram constructed from chemical or mineralogical data on representative samples. The diagram shows the proportion of the variance in each constituent that can be accounted for by mixing models with any given number of end members. It is unlikely that the relatively simple compositional structures revealed for some rock bodies arose by chance, even though statistical tests for this likelihood are not available. Factor-variance diagrams constructed for a wide range of igneous masses reveal an equally wide range of compositional structures.

A rock body that is highly variable in composition can have either a simple or complex compositional structure, and one that is nearly homogeneous, similarly, can be of either simple or complex compositional structure. The compositional structure is determined by the simplicity or complexity of the combination of processes that caused the compositional variation—not by the amount of variation present. In fact, if an igneous body were perfectly homogeneous throughout, the only observed compositional variation would be that caused by analytical errors, and the compositional structure would probably appear to be quite complex. This would be particularly true if the analytical errors for the various oxides tended to be independent of each other.

The possibility should not be overlooked that the compositional structure within a magma might have been totally eradicated by thorough homogenization before the magma solidified. This could result, perhaps, from diffusion and convection operating over long periods of time. Such homogenization may have occurred in some magmas, but the fact that it does not occur in all of them is substantiated by the simple compositional structures that some of them display, and by the large-scale compositional variations that are present. Homogenization could not have been an important factor in the Sierra Nevada and Alaska-Aleutian Range batholiths, which are composed of plutonic sequences that differ in age by as much as 100 million years (Bateman and Dodge, 1970, p. 419; Reed and Lanphere, 1969, p. 39–41; 1973, p. 2605).

Factor-variance diagrams representing the batholiths of the Sierra Nevada and the Alaska-

TABLE 21.—*Data pertaining to points within tetrahedrons of figure 14*

Group of plutons	Point in fig. 14	Percent Q+Or+Ab+An in melt	Position of point in tetrahedron				Percent melting	Percent mafic assemblages retained in (+) or precipitated from (−) melt
			Q	Or	Ab	An		
White Mountains rocks (fig. 14*A*)	*z*	92.6	29	70	1	0	11.2	+22.8
Do	*x*	96.5	25	23	45	7	27.0	+8.5
Do	*a*	97.3	28	40	31	1	17.1	+8.3
Do	*b*	93.8	24	36	32	8	20.0	+5.4
Do	*c*	80.5	10	22	39	30	40.0	−14.6
Do	*d*	73.4	1	13	43	43	80.0	−54.6
Do	*m*	72.8	0	11	43	46	100.0	−74.6
Palisade Crest sequence (fig. 14*B*)	*z*	94.5	37	58	5	0	11.8	+6.6
Do	*x*	96.9	30	26	38	5	22.5	+7.2
Do	*a*	97.5	34	38	27	1	16.5	+9.9
Do	*b*	93.3	28	33	29	10	20.0	+6.4
Do	*c*	80.4	12	20	37	31	40.0	−13.6
Do	*d*	74.1	3	12	43	43	80.0	−53.6
Do	*m*	72.1	0	10	43	47	100.0	−73.6
Scheelite sequence (fig. 14*C*)	*z*	97.3	44	43	13	0	13.5	+15.2
Do	*x*	97.1	35	26	34	5	20.8	−0.5
Do	*a*	97.6	39	33	25	2	16.7	+4.2
Do	*b*	93.7	33	29	27	10	20.0	+0.9
Do	*c*	80.7	15	18	36	31	40.0	−19.1
Do	*d*	73.6	4	11	42	44	80.0	−59.1
Do	*m*	72.2	1	9	43	47	100.0	−79.1
Toulumne intrusive series (fig. 14*D*)	*z*	97.4	37	33	27	3	17.3	+1.2
Do	*x*	95.9	26	9	54	12	46.3	+16.3
Do	*a*	97.0	34	26	35	5	21.2	+5.6
Do	*c*	83.2	16	17	39	28	40.0	−13.2
Do	*d*	77.8	7	9	45	38	80.0	−53.2
Do	*m*	72.2	1	9	43	47	100.0	−73.2
Yosemite rocks (figure 14*E*)	*z*	97.2	39	26	30	5	19.3	−0.4
Do	*x*	96.6	33	17	42	9	27.6	+4.0
Do	*a*	97.1	38	24	32	6	20.7	+2.1
Do	*c*	83.0	18	16	37	29	40.0	−17.2
Do	*d*	74.9	6	10	42	42	80.0	−57.2
Do	*m*	72.3	2	9	42	47	100.0	−77.2
Shaver sequence (figure 14*F*)	*z*	97.0	46	44	9	0	12.9	+35.5
Do	*x*	97.0	37	26	32	5	23.6	+7.5
Do	*a*	97.2	39	29	28	4	18.1	+5.8
Do	*b*	95.0	35	27	29	8	20.0	+4.0
Do	*c*	81.5	16	17	36	31	40.0	−16.1
Do	*d*	73.8	4	10	41	44	80.0	−56.1
Do	*m*	72.3	2	9	43	47	100.0	−76.1

Aleutian Range reveal compositional structures that are relatively simple. More than 90 percent of the variance in each major oxide can be accounted for by mixing three end members in the case of the Alaska-Aleutian Range, and four in the case of the Sierra Nevada. There is no purely mathematical means for determining what the end members were, although proposed end-member compositions can be tested and

possibly rejected. Testing consists of determining the compatibility of the proposed composition with the compositional series formed by the representative samples, through estimation of a vector communality, and through determination and consideration of the mixing proportions required when that end-member composition is used in combination with others to form the mixing model.

The major implication of the models for the batholiths is that both could have originated from magmas or magma-source materials with andesitic compositions. Moreover, the models indicate that modification of the magmas, or of the magma-source material, could have been accomplished almost entirely by the separation of mafic mineral assemblages similar in composition to the mafic inclusions that are scattered throughout most of the granitic rocks or to mafic phases within these rocks. The mafic mineral assemblages could have consisted of minerals precipitated from the magmas or of refractory minerals in the magma-source materials.

If the Alaska-Aleutian Range batholith originated from partial melting, the minimum degree of melting required by the model ranges from about 5.6 to 23.7 percent for the 158 samples. The average sample could have formed with as little as 9.0 percent melting if 3.9 percent of the refractory material were retained in the melt. The model for the Sierra Nevada batholith indicates that all but one of the individual 228 samples could have formed with melting in the range from 11 to 27 percent. The average sample from each group of plutons could have formed with as little as 16.5 to 21.2 percent melting if 2.1 to 9.9 percent of the refractory material were retained. In a general way, groups of plutons within the Alaska-Aleutian Range batholith distant from the continental margin could have resulted from lower degrees of melting than those closer to the margin. If data from experimental petrology are applicable, the melts that formed the eastermost plutons in the Sierra Nevada batholith may have undergone higher partial pressures of H_2O than did those closer to the continental margin.

The compositional structures of the batholiths indicate that three end members can account for most of the compositional variation in each batholith, and that the addition of a fourth end member to the Sierra Nevada model can improve this model substantially. If the batholiths formed from starting materials from which materials of varying composition were separated, at least three end members are required. Processes of magma mixing and assimilation would require additional end members in the models, which would contradict the determined compositional structures. It is concluded that these processes and others could not have been quantitatively important in causing compositional variation in either batholith.

The two models leave less than 10 percent of the variance in each oxide constituent unexplained. The remaining variance could be attributed to rock-forming processes not represented in the models, to compositional variations in the proposed end members, and to analytical imprecision. Those who may have little feeling for what this means in terms of original data versus data computed from the models may refer to table 22. Table 22 shows the determined mixing proportions for every tenth sample from the Alaska-Aleutian Range, the compositions reported by Reed and Lanphere (1974) (recalculated to sum to 100 percent), and the compositions computed for the indicated mixture of end members. A similar comparison of original and model data for the Sierra Nevada batholith shows even better agreement than indicated in table 22 because, as shown in table 5, all of the variances not accounted for by the Sierra Nevada four-end-member model are considerably smaller than those for the Alaska-Aleutian Range three-end-member model.

It has been assumed that both batholiths are of magmatic origin and that the compositional variations in each were brought about by differential separation of mafic mineral assemblages. This has led to hypothetical end-member compositions which might have been involved in the formation of the two batholiths. Although speculative, each model is one example that shows how knowledge of the compositional structures can serve to form and test the quantitative aspects of petrologic models. The primary intent of this report, however, has been to present the concept of compositional structure and to show the relatively simple compositional structures of the two batholiths of circumpacific North America. If the models can withstand the critical scrutiny of theoretical petrologists and other geologists who have studied the Sierra Nevada and the Alaska-Aleutian Range, they show that each batholith could have formed by a rather simple combination of processes. Even though the models may be rejected on valid grounds by other investigators, alternative models will have to be reconciled with the fact that both batholiths have simple compositional structures that call for three principal end members in any model that might be proposed.

APPENDIX

The preliminary *Q*-mode factor analyses of the chemical data for both batholiths were made with the CABFAC computer program of Klovan and Imbrie (1971) as extended for treatment of compositional data by Klovan and Miesch (1976). The extended CABFAC program provided the data for the construction of the

TABLE 22.—*Mixing proportions, original data, and corresponding data generated from the Alaska-Aleutian Range batholith model for selected samples*

[Original data are from Reed and Lanphere (1974, table 1) although total iron has been recomputed as 'FeO' and the seven major oxides have been recalculated to sum to 100]

Sample No.	Mixing proportions[1]				Chemical compositions (weight percent)						
	MGM	*ABH*	*ANH*		SiO_2	Al_2O_3	'FeO'	MgO	CaO	Na_2O	K_2O
10	9.9150	−5.7953	−3.1198	Original	74.46	13.80	2.35	0.38	1.63	4.02	3.35
				Model	74.25	14.52	1.72	.24	1.42	3.99	3.71
20	11.0061	−6.6850	−3.3211	Original	75.11	13.36	2.01	.40	1.42	3.75	3.95
				Model	75.06	14.00	1.66	.20	1.02	3.68	4.22
30	5.4280	−2.5472	−1.8808	Original	67.13	17.19	3.70	1.54	3.99	4.50	1.94
				Model	66.99	17.04	3.68	1.56	4.23	4.51	1.92
40	4.9029	−2.4060	−1.4969	Original	64.15	17.63	5.00	2.36	4.92	4.10	1.84
				Model	63.87	17.53	4.91	2.39	5.23	4.13	1.87
50	5.1199	−2.3995	−1.7204	Original	66.13	17.55	4.17	1.43	4.59	4.29	1.84
				Model	65.78	17.27	4.13	1.87	4.63	4.41	1.84
60	4.9021	−2.2687	−1.6334	Original	63.67	18.34	5.32	1.34	4.22	4.74	2.37
				Model	65.17	17.42	4.34	2.01	4.84	4.38	1.78
70	3.4817	−1.6053	−0.8764	Original	59.10	17.79	7.16	3.48	6.95	4.09	1.43
				Model	59.41	18.52	6.48	3.45	6.75	3.87	1.46

[1]See table 12 for compositions of end members *MGM*, *ABH*, and *ANH*.

factor-variance diagrams in figures 3–5 and 7–8 and produced output files containing other selected results from each *Q*-mode analysis. All further computations were performed using the interactive programs described in Miesch (1976c). The output file from the extended CABFAC program was transformed to another output file with program EQTRAN. The transformed output file was then used as input to the other interactive programs.

Program EQSPIN was used to derive the stereograms in figures 9 and 10, and program EQSTER was used to determine the compositions represented by vectors at various positions on the stereograms. (See, for example, tables 8 and 9.) Program EQEXAM was used to examine individual compositions, such as the compositions of selected minerals, for compatibility with the compositional series formed by the sample compositions when represented in three- or four-dimensional vector systems; compatibility is indicated by the projected vector communality. The compositional system formed by hornblende-albite-anorthite-magnetite (fig. 11) was examined for each batholith with program EQSCAN. After the points *Y* and *Z* were located on the stereograms of figures 9 and 10, point *MGM* on each stereogram was determined with program INSECT. The compositions of the end members and the corresponding CIPW norms (tables 11, 12, and 15) were determined with program EQMAIN. EQMAIN also provided the mixing proportions (composition loadings) summarized in tables 13, 14, and 16. The final checks on the computations, as represented in table 22, were made with program EQCHEK.

Examination of the ranges of possible melt compositions called for by the models (figures 13 and 14; tables 20 and 21) was made with other computer programs that have not been published. The methods of computation, however, are fully outlined in table 19.

REFERENCES CITED

Barker, F., Wones, D. R. Sharp, W. N., and Desborough, G. A., 1975, The Pikes Peak batholith, Colorado Front Range, and a model for the origin of the gabbro-anorthosite-syenite-potassic granite suite: Precambrian Research, v. 2, p. 97–160.

Bateman, P. C., Clark, L. D., Huber, N. K., Moore, J. G., and Rinehart, C. D., 1963, The Sierra Nevada batholith—a synthesis of recent work across the central part: U.S. Geol. Survey Prof. Paper 414-D, 46 p.

Bateman, P. C., and Dodge, F. C., 1970, Variations of major chemical constituents across the central Sierra Nevada batholith: Geol. Soc. America Bull., v. 81, no. 2, p. 409–420.

Bryan, W. B., Finger, L. W., and Chayes, F., 1969. Estimating proportions in petrographic mixing equations by least squares approximation: Science, v. 163, no. 3870, p. 926–927.

Carden, J. R., and Laughlin, A. W., 1974, Petrochemical variations within the McCartys basalt flow, Valencia County, New Mexico: Geol. Soc. America Bull., v. 85, no. 9, p. 1479–1484.

Carmichael, I. S. E., Turner, F. J., and Verhoogen, John, 1974, Igneous Petrology: New York, McGraw-Hill Book Co., 739 p.

Dodge, F. C. W., Papike, J. J., and Mays, R. E., 1968, Hornblendes from granitic rocks of the central Sierra Nevada batholith, California: Jour. Petrology, v. 9, pt. 3, p. 378–410.

Fenner, C. N., 1938, Contact relations between rhyolite and basalt on Gardiner River, Yellowstone Park, Geol. Soc. America Bull., v. 49, p. 1441–1484.

Imbrie, John, 1963, Factor and vector analysis programs for analyzing geologic data: U.S. Office Naval Research, Geog. Branch Tech. Rept. 6, ONR Task No. 389-135, 83 p.

James, R. S., and Hamilton, D. L., 1969, Phase relations in the system $NaAlSi_3O_8$-$KAlSi_3O_8$-$CaAl_2Si_2O_8$-SiO_2 at 1 kilobar water vapour pressure: Contr. Mineralogy and Petrology, v. 21, p. 111-141.

Kaiser, H. F., 1958, The varimax criterion for analytical rotation in factor analysis: Psychometrika, v. 23, p. 187-200.

Kistler, R. W., and Peterman, Z. E., 1973, Variations in Sr, Rb, K, Na, and initial Sr^{87}/Sr^{86} in Mesozoic granitic rocks and intruded wall rocks in central California: Geol. Soc. America Bull., v. 84, no. 11, p. 3489-3512.

Klovan, J. E., 1975, *R*- and *Q*-mode factor analysis, *in* R.B. McCammon, ed., Concepts in Geostatistics: New York, Springer-Verlag, Inc., p. 21-69.

Klovan, J. E., and Imbrie, John, 1971, An algorithm and FORTRAN-IV program for large scale *Q*-mode factor analysis and calculation of factor scores: Internat. Assoc. for Mathematical Geology Jour., v. 3, no. 1, p. 61-77.

Klovan, J. E., and Miesch, A. T., 1976, Extended CABFAC and QMODEL computer programs for *Q*-mode factor analysis of compositional data: Computers and Geosciences, v. 1, no. 3, p. 161-178.

Lee, D. E., and Van Loenen, R. E., 1971, Hybrid granitoid rocks of the southern Snake Range, Nevada: U.S. Geol. Survey Prof. Paper 668, 48 p.

Luth, W. C., Jahns, R. H., and Tuttle, O. F., 1964, The granite system at pressures of 4 to 10 kilobars: Jour. Geophys. Research, v. 69, no. 4, p. 759-773.

Manson, Vincent, and Imbrie, John, 1964, FORTRAN program for factor and vector analysis of geologic data using an IBM 7090 or 7094/1401 computer system: Kansas Geol. Survey Spec. Distrib. Pub. 13, 46 p.

Miesch, A. T., 1976a, *Q*-mode factor analysis of compositional data: Computers and Geosciences, v. 1, no. 3, p. 147-159.

_____1976b, *Q*-mode factor analysis of geochemical and petrologic data matrices with constant row-sums: U.S. Geol. Survey Prof. Paper 574-G, 47 p.

_____1976c, Interactive computer programs for petrologic modeling with extended *Q*-mode factor analysis: Computers and Geosciences, v. 2, no. 4, p. 439-492.

Miesch, A. T., and Morton, D. M., 1977, Chemical variability in the Lakeview Mountains pluton, southern California batholith—A Comparison of the methods of correspondence analysis and extended *Q*-mode factor analysis: U.S. Geol. Survey Jour. Research, v. 5, no. 1, p. 103-116.

Moore, J. G., 1959, The quartz diorite boundary line in the western United States: Jour. Geology, v. 67, no. 2, p. 198-210.

Morton, D. M., Baird, A. K., and Baird, K. W., 1969, The Lakeview Mountains pluton, southern California batholith, pt. II—Chemical composition and variation: Geol. Soc. America Bull., v. 80, no. 8, p. 1553-1564.

Murata, K. J., and Richter, D. H., 1966, Chemistry of the lavas of the 1959-1960 eruption of Kilauea Volcano, Hawaii: U.S. Geol. Survey Prof. Paper 537-A, 26 p.

Nockolds, S. R., 1954, Average chemical compositions of some igneous rocks: Geol. Soc. America Bull., v. 65, no. 10, p. 1007-1032.

Nockolds, S. R., and Mitchell, R. L., 1946, The geochemistry of some Caledonian plutonic rocks—a study in the relationship between major and trace elements of igneous rocks and their minerals: Royal Soc. Edinburgh Trans., v. 61, p. 533-575 [1948].

Presnall, D. C., and Bateman, P. C., 1973, Fusion relations in the system $NaAlSi_3O_8$-$CaAl_2Si_2O_8$-$KAlSi_3O_8$-SiO_2-H_2O and generation of granitic magmas in the Sierra Nevada batholith: Geol. Soc. America Bull., v. 84, no. 10, p. 3181-3202.

Reed, B. L., and Lanphere, M. A., 1969, Age and chemistry of Mesozoic and Tertiary plutonic rocks in south-central Alaska: Geol. Soc. America Bull., v. 80, no. 1, p. 23-43.

_____1973, Alaska-Aleutian Range batholith—Geochronology, chemistry and relation to circum-Pacific plutonism: Geol. Soc. America Bull., v. 84, no. 8, p. 2583-2610.

_____1974, Chemical variations across the Alaska-Aleutian Range batholith: U.S. Geol. Survey Jour. Research, v. 2, no. 3, p. 343-354.

Wager, L. R., and Brown, G. M., 1968, Layered igneous rocks: Edinburgh and London, Oliver and Boyd, Ltd., 588 p.

Wright, W. H., III, 1975, The Stanislaus River; a study in Sierra Nevada geology: California Geology, v. 28, no. 1, p. 3-10.

* U.S. GOVERNMENT PRINTING OFFICE: 1979--0-677-026/45